



19 **Abstract**

20 **In addition to woody and herbaceous plants, mosses are ubiquitous in northern terrestrial**  
21 **ecosystems, which play an important role in regional carbon, water and energy cycling.**  
22 **Current global land surface models that do not considering moss may bias the**  
23 **quantification of the regional carbon dynamics. Here we incorporate moss into a process-**  
24 **based biogeochemistry model, the Terrestrial Ecosystem Model (TEM 5.0), as a new plant**  
25 **functional type to develop a new model (TEM\_Moss). The new model explicitly quantifies**  
26 **the interactions between vascular plants and mosses and their competition for energy,**  
27 **water, and nutrients. Compared to the estimates using TEM 5.0, the new model estimates**  
28 **that the regional terrestrial soils store 132.7 Pg more C at present day, and will store 157.5**  
29 **Pg and 179.1 Pg more C under the RCP 8.5 and RCP 2.6 scenarios, respectively, by the end**  
30 **of the 21<sup>st</sup> century. Ensemble regional simulations forced with different parameters for the**  
31 **21<sup>st</sup> century with TEM\_Moss predict that the region will accumulate 161.1±142.1 Pg C**  
32 **under the RCP 2.6 scenario, and 186.7±166.1 Pg C under the RCP 8.5 scenario over the**  
33 **century. Our study highlights the necessity of coupling moss into Earth System Models to**  
34 **adequately quantify terrestrial carbon-climate feedbacks in the Arctic.**

35

36

37

38

39

## 40 **1. Introduction**

41 Northern high latitude ecosystems, which refers to the land ecosystems (>45 °N) in  
42 northern temperate, boreal, grassland and tundra regions, hold about 30% of global terrestrial  
43 carbon (C) in soils and plants (Allison and Treseder, 2008; Jobbágy and Jackson, 2000;  
44 Kasischke, 2000; Tarnocai et al., 2009; Hugelius et al., 2014), and contain as much as 1024 Pg  
45 soil organic carbon from 0 to 3 m depth (Treseder et al., 2016; Schuur et al., 2008). This large  
46 amount of carbon is potentially responsive to ongoing global warming (Burke et al., 2017,  
47 Koven et al., 2015, Comyn-Platt et al., 2018)), which is especially pronounced at high latitudes  
48 (Treseder et al., 2016; IPCC, 2014). Thus, explicit investigation of carbon-climate feedback is  
49 important (Wieder et al., 2013; Bond-Lamberty and Thomson, 2010).

50 Ecosystem models are important tools for understanding the role of boreal ecosystems in  
51 carbon-climate feedbacks (Bond-Lamberty et al., 2005; Chadburn et al., 2017; Zhuang et al.,  
52 2002; Treseder et al., 2016). Process-based biogeochemical models such as TEM (Hayes et al.,  
53 2014; Raich et al., 1991; Melillo et al., 1993; McGuire et al., 1992; Zhuang et al., 2001, 2002,  
54 2010, 2013), Biome-BGC (Running and Coughlan, 1988; Bond-Lamberty et al., 2007), and  
55 Biosphere Energy Transfer Hydrology scheme (BETHY) (Knorr, 2000) are increasingly  
56 employed to simulate current and future carbon dynamics. Those models estimate carbon  
57 dynamics by simulating processes such as photosynthesis, respiration, nitrogen competition,  
58 evapotranspiration and soil decomposition (Bond-Lamberty et al., 2005; Zhuang et al., 2015).  
59 The results from these models are influenced by components and processes that are built into the  
60 model (Turetsky et al., 2012; Oreskes et al., 1994). However, the role of boreal forests in carbon  
61 sink or source activities has not yet reached a consensus due to a number of model limitations  
62 (Cahoon et al., 2012; Hayes et al., 2011; Todd-Brown et al., 2013).

63           One limitation is that ecosystems models often ignore some important components such  
64 as understory processes that play crucial roles in biogeochemical cycles (Zhuang et al., 2002;  
65 Treseder et al., 2011; Bond-Lamberty et al., 2005). For instance, mosses are ubiquitous in  
66 northern ecosystems, and show a pattern of increasing abundance with increasing latitude  
67 (Turetsky et al., 2012; Jägerbrand et al., 2006). Their functional traits, including tolerance to  
68 drought and a broad response of net assimilation rates to temperature, allow them to persist in  
69 high-latitude regions (Kallio and Heinonen, 1975; Harley et al., 1989). The activities of moss  
70 that are related to water, nutrients, and energy may influence several ecosystem processes such  
71 as permafrost formation and thaw, peat accumulation, soil decomposition and net primary  
72 productivity (NPP) (Turetsky et al., 2012; Nilsson and Wardle, 2005). Mosses can have positive  
73 or negative interactions with vascular plants (Skre and Oechel, 1979; Turetsky et al., 2010). On  
74 the one hand, mosses compete with vascular plants for available nutrients, negatively affecting  
75 vascular plants productivity (Skre and Oechel, 1979; Gornall et al., 2011; Turetsky et al., 2012).  
76 Besides, a thick moss cover can form an environment with water logging or low oxygen supply,  
77 which is common in high-latitude regions (Skre and Oechel, 1979; Cornelissen et al., 2007). The  
78 moss cover prevents absorbed solar heat from being conducted down into the soil, and tends to  
79 decrease soil temperature in summer. Therefore, soil decomposition rates can be affected since  
80 they are mediated by soil temperature, which will further influence growth of vascular plants  
81 (Gornall et al., 2007). On the other hand, some species of mosses can serve as an important  
82 source of nitrogen because of their associations with microbial nitrogen fixers (Basilier, 1979;  
83 DeLuca et al., 2007; Markham, 2009; Kip et al., 2011). Thus, mosses can also exert positive  
84 effects on plant growth due to their regulation of nitrogen availability for vascular plants (Hobbie  
85 et al., 2000; Gornall et al., 2007). It is gradually being recognized that mosses can have

86 comparable influences on high-latitude ecosystems to vascular plants, due to their large density  
87 and essential function in plant competition, soil climate, and carbon and nutrient cycling  
88 (Longton, 1988; Lindo and Gonzalez, 2010; Okland, 1995; Pharo and Zartman, 2007). They can  
89 on average contribute 20% of aboveground NPP in boreal forests (Turetsky et al., 2010), and  
90 their annual NPP may reach as high as 350 g C m<sup>-2</sup> in some regions in the Arctic (Pakarinen and  
91 Vitt 1973), even exceeding that of vascular plants (Oechel and Collins, 1976; Clarke et al.,  
92 1971). Thus, ignorance of mosses, the keystone species of boreal ecosystems, can pose large  
93 biases in model predictions and limit the utility of models. To date, a number of ecosystem  
94 models have already included moss activities to explore the response of moss to disturbance  
95 (Bond-Lamberty et al., 2007; Euskirchen et al., 2009; Frohking et al., 2010, Wania et al., 2009,  
96 Chadburn et al., 2015, Porada et al., 2016, Druel et al., 2017), or improve model prediction of  
97 carbon dynamics (Bond-Lamberty et al., 2005). However, the potential role of moss in the  
98 regional carbon dynamics in northern high latitudes has been slowly evaluated by considering  
99 the interactions between moss and vascular plants, especially with respect to their competition  
100 for water, nutrient and energy.

101 This study developed a new version of Terrestrial Ecosystem Model (Raich et al., 1991;  
102 McGuire et al., 1992; Zhuang et al., 2001, 2002, 2010, 2013, 2015), hereafter referred to as  
103 TEM\_Moss, by explicitly considering moss impacts on terrestrial ecosystem carbon dynamics.  
104 The competition of water, energy and nutrient between vascular plants and mosses are explicitly  
105 modeled. The verified TEM\_Moss and previous TEM were compared against the observed data of  
106 ecosystem carbon, soil temperature and moisture dynamics. Both models were then used to analyze  
107 the regional carbon dynamics in northern high latitudes (north of 45 °N) during the 20<sup>th</sup> and 21<sup>st</sup>  
108 centuries.

## 109 **2. Methods**

### 110 **2.1 Overview**

111 First, we briefly describe how we developed the TEM\_Moss by modifying the previous  
112 TEM 5.0 to consider their interactions between vascular plants and mosses. Second,  
113 parameterization and validation of TEM\_Moss using measured gap-filled carbon flux data and  
114 meteorological data at representative sites is presented. Third, we present how we have applied  
115 both models (TEM\_Moss and TEM 5.0) to the northern high latitudes (above 45 °N) to quantify  
116 regional carbon dynamics during the 20<sup>th</sup> and 21<sup>st</sup> centuries.

### 117 **2.2 Model description**

118 TEM is a process-based, large-scale biogeochemical model that uses monthly climatic data  
119 and spatially explicit vegetation and soil information to simulate the dynamics of carbon and  
120 nitrogen fluxes and pool sizes of plants and soils (Raich et al., 1991; McGuire et al., 1992; Zhuang  
121 et al., 2010, 2015, 2020). However, in previous versions of TEM, the interactions between mosses  
122 and vascular plants on carbon and nitrogen cycling have not been included. Here we developed a  
123 TEM\_Moss model by modifying model structure and incorporating activities of moss into extant  
124 TEM 5.0 (Zhuang et al., 2003). Based on the structure of TEM 5.0, we added carbon and nitrogen  
125 pools and fluxes to simulate activities of moss including photosynthesis, respiration, litterfall and  
126 nutrient and water cycling (Figure 1). Thus, the structure of TEM\_Moss includes the processes of  
127 both vascular plants and mosses (Figure 1).

128 In TEM\_Moss, moss photosynthesis ( $GPP_m$ ) is described as a maximum rate, reduced by  
129 influence of photosynthetically active radiation, mean air temperature, mean atmospheric carbon

130 dioxide concentrations, moss moisture, and indirectly, nitrogen availability (Frolking et al., 1996;  
131 Launiainen et al., 2015; Zhuang et al., 2002). For each time step,  $GPP_m$  is calculated as:

$$132 \quad GPP_m = C_{max} * f(PAR) * f(T) * f(w_m) * f([CO_2]) * f(NA) \quad (1)$$

133 where  $C_{max}$  denotes the maximum rate of carbon assimilation by moss (units:  $gC\ m^{-2}mon^{-1}$ ),  
134  $f(PAR)$  is a scalar function that depends on monthly photosynthetically active radiation (PAR),  
135 which is calculated as (Frolking et al., 1996; Launiainen et al., 2015; Kulmala et al., 2011):

$$136 \quad f(PAR) = \frac{PAR}{b+PAR} \quad (2)$$

137 where  $b$  (units:  $\mu mol\ m^{-2}\ s^{-1}$ ) is the half saturation constant for PAR use by moss as indicated by  
138 the Michaelis–Menten kinetic.

139 The temperature effect on moss photosynthesis is modeled as a multiplier (Frolking et al.,  
140 1996; Raich et al., 1991):

$$141 \quad f(T) = \frac{(T-T_{min})*(T-T_{max})}{(T-T_{min})*(T-T_{max})-(T-T_{opt})^2} \quad (3)$$

142 where  $T$  is the monthly mean air temperature (units:  $^{\circ}C$ ), and  $T_{min}$ ,  $T_{max}$ , and  $T_{opt}$  are parameters  
143 (units:  $^{\circ}C$ ) that limit  $f(T)$  to a range of zero to one.

144 The moisture effect is also modeled as a multiplier (Frolking et al., 1996; Raich et al.,  
145 1991):

$$146 \quad f(w_m) = \frac{(w_m-w_{min})*(w_m-w_{max})}{(w_m-w_{min})*(w_m-w_{max})-(w_m-w_{opt})^2} \quad (4)$$

147 where  $w_m$  is moss moisture (units: mm), and  $w_{min}$ ,  $w_{max}$ , and  $w_{opt}$  are related parameters (units:  
148 mm) that limit  $f(w_m)$  to a range of zero to one.

149  $f([\text{CO}_2])$  is also a scalar function that depends on monthly mean atmospheric carbon  
150 dioxide concentration (Zhuang et al., 2002; Raich et al., 1991):

$$151 \quad f([\text{CO}_2]) = \frac{[\text{CO}_2]}{k_m + [\text{CO}_2]} \quad (5)$$

152 where  $[\text{CO}_2]$  (units:  $\mu\text{L/L}$ ) represents monthly mean atmospheric carbon dioxide concentration,  
153 the  $k_m$  (units:  $\mu\text{L/L}$ ) is the internal  $\text{CO}_2$  concentration at which moss C assimilation proceeds at  
154 one-half its maximum rate.

155 The function  $f(\text{NA})$  models the limiting effects of plant nitrogen status on GPP (McGuire  
156 et al., 1992; Zhuang et al., 2002), which is a scalar function that depends on monthly N available  
157 for incorporation into plant production of new tissue.

158 Meanwhile, in TEM\_Moss, we defined the moss respiration rate ( $R_m$ ) as a function of  
159 moss respiration rate at 10 °C, moss respiration temperature sensitivity which was expressed as a  
160  $Q_{10}$  function, and moss moisture (Launiainen et al., 2015; Frohking et al., 1996):

$$161 \quad R_m = R_{10,m} * Q_{10,m}^{\frac{T_m - 10}{10}} * f^*(w_m) \quad (6)$$

162 where  $R_{10,m}$  (units:  $\text{gC m}^{-2}\text{mon}^{-1}$ ) represents the moss respiration rate at 10 °C, the parameter  
163  $Q_{10,m}$  is moss respiration temperature sensitivity,  $T_m$  is moss temperature (°C) and  $w_m$  is moss  
164 moisture (mm).

165 The function  $f^*(w_m)$  denotes the moisture effect on moss respiration. Here we used  
166  $f^*(w_m)$  to distinguish with the function  $f(w_m)$ , which is moisture effect on moss  
167 photosynthesis as mentioned earlier.  $f^*(w_m)$  is defined as (Frohking et al., 1996; Zhuang et al,  
168 2002):



169 
$$f^*(w_m) = 1 - \frac{(w_m - w_{\min} - w_{\text{opt},r})^2}{(w_m - w_{\min}) * w_{\text{opt},r} + w_{\text{opt},r}^2} \quad (7)$$

170 where  $w_{\text{opt},r}$  (units: mm) denotes the optimal water content for moss respiration.

171 Besides, the carbon in litter production from mosses to soil ( $L_{C,m}$ ) is modeled as  
 172 proportional to moss carbon biomass with a constant ratio (Zhuang et al., 2002):

173 
$$L_{C,m} = c_{\text{fall}_m} * \text{MOSSC} \quad (8)$$

174 where MOSSC denotes the moss carbon biomass, and  $c_{\text{fall}_m}$  is the corresponding constant  
 175 proportion.

176 Thus, the change of moss carbon pool (MOSSC) can be modeled as:

177 
$$\frac{d\text{MOSSC}}{dt} = \text{GPP}_m - R_m - L_{C,m} \quad (9)$$

178 On the other hand, researches have shown that mosses can uptake substantial inorganic  
 179 nitrogen from the bulk soil (Ayres et al., 2006, Fritz et al., 2014). In our model, nitrogen uptake  
 180 by moss ( $N_{\text{uptake}_m}$ ) is modelled as a function of available soil nitrogen, moss moisture, and  
 181 mean air temperature, and the relative amount of energy allocated to N versus C uptake (Zhuang  
 182 et al., 2002; Raich et al., 1991):

183 
$$N_{\text{uptake}_m} = N_{\text{max}} * \frac{K_s * N_{\text{av}}}{k_n + K_s * N_{\text{av}}} * e^{0.0693T} * (1 - A_m) \quad (10)$$

184 Where  $N_{\text{max}}$  is the maximum rate of nitrogen uptake by mosses (units:  $\text{gC m}^{-2}\text{mon}^{-1}$ ), and  $N_{\text{av}}$   
 185 (units:  $\text{g m}^{-2}$ ) represents available soil nitrogen, which is treated as a state variable in our model.  
 186  $k_n$  (units:  $\text{g m}^{-2}$ ) is the concentration of available soil nitrogen at which nitrogen uptake proceeds  
 187 at one-half its maximum rate.  $T$  is the monthly mean air temperature ( $^{\circ}\text{C}$ ), and  $A_m$  is a unitless  
 188 parameter ranging from 0 to 1, which represents relative allocation of effort to carbon vs.

189 nitrogen uptake.  $K_s$  is a parameter accounting for relative differences in the conductance of the  
 190 soil to N diffusion, which can be calculated through moss moisture (Zhuang et al., 2002; Raich et  
 191 al., 1991):

$$192 \quad K_s = 0.9 * \left(\frac{w_m}{w_f}\right)^3 + 0.1 \quad (11)$$

193 where  $w_f$ (units: mm) denotes the moss field capacity.

194 The nitrogen in litter production from mosses to soil ( $L_{N,m}$ ) is modeled as proportional to  
 195 moss nitrogen biomass with a constant ratio (Zhuang et al., 2002):

$$196 \quad L_{N,m} = nfall_m * MOSSN \quad (12)$$

197 where  $nfall_m$  is the constant proportion to moss nitrogen biomass (MOSSN).

198 Thus, the changes in moss nitrogen pool (MOSSN) can be modeled as:

$$199 \quad \frac{dMOSSN}{dt} = Nuptake_m - L_{N,m} \quad (13)$$

200 At the same time, total carbon and nitrogen in litterfall, and total nitrogen uptake from  
 201 soil available nitrogen are changed due to incorporation of mosses:

$$202 \quad Litterfall_C = L_{C,v} + L_{C,m} \quad (14)$$

$$203 \quad Litterfall_N = L_{N,v} + L_{N,m} \quad (15)$$

$$204 \quad Nuptake = Nuptake_v + Nuptake_m \quad (16)$$

205 Where  $L_{C,v}$  and  $L_{N,v}$  are carbon and nitrogen in litter production from vascular plants to soil, and  
 206  $Nuptake_v$  is nitrogen uptake by vascular plants (Raich et al., 1991; Melillo et al., 1993; Zhuang  
 207 et al., 2003).

208 Except above equations, other governing equations in TEM 5.0 have not been changed.  
209 More equations of TEM 5.0 have been documented in previous studies (Raich et al., 1991;  
210 McGuire et al., 1992; Zhuang et al., 2003; Zha and Zhuang, 2018).

211 In TEM 5.0, a soil thermal module (STM) simulates soil thermal dynamics considering  
212 the effects of moss thickness, soil moisture, and snowpack (Zhuang et al., 2001, 2002). In STM,  
213 soil profile was treated as a three soil-layer system: (1) a moss plus fibric soil organic layer, (2) a  
214 humic organic soil layer, and (3) a mineral soil layer, and temperature for each layer can be  
215 derived from STM (Zhuang et al., 2001, 2002, 2003). Temperature in moss layer is estimated  
216 with STM.

217 A water balance module (WBM) was also incorporated into TEM 5.0 to simulate soil  
218 hydrologic dynamics (Vörösmarty et al., 1989; Zhuang et al., 2001). The WBM receives  
219 information on precipitation, air temperature, potential evapotranspiration, vegetation, soils and  
220 elevation to predict soil moisture evapotranspiration and runoff (Vörösmarty et al., 1989). The  
221 whole soil was treated as a single profile in WBM (Vörösmarty et al., 1989; Zhuang et al., 2001).  
222 To simulate moss moisture, we added a moss layer on the soil profile by modifying the WBM  
223 (Figure 2). Similar to soil moisture, moss moisture is also treated as a state variable in the revised  
224 WBM, which is modeled as:

$$225 \quad \frac{dw_m}{dt} = \text{snowfall} + \text{rainfall} - \text{percolation} - \text{moss evapotranspiration} \quad (17)$$

226 where the term “percolation” denotes the percolation from moss, which is the sum of rainfall  
227 percolation and snowmelt percolation from moss. We assume that there is no runoff from moss  
228 layer.

229 Accompanied by the above equation, changes in soil water (SM) is modified as:

230 
$$\frac{dSM}{dt} = \text{percolation} - \text{rain excess} - \text{snow excess} - \text{plant evapotranspiration} \quad (18)$$

231 Calculations for these water fluxes regarding vascular plants were not changed. More details  
232 about an earlier version of WBM were described in Vörösmarty et al. (1989) and Zhuang et al.  
233 (2001).

### 234 **2.3 Model parameterization and validation**

235 The newly introduced parameters that are associated with moss activities were documented  
236 in Table 1. We parameterized the TEM\_Moss for six representative ecosystem types in northern  
237 high latitudes with gap-filled monthly net ecosystem productivity (NEP,  $\text{gCm}^{-2}\text{mon}^{-1}$ ) data from  
238 the AmeriFlux network (Davidson et al., 2000). We assumed that the moss types are associated  
239 with the representative ecosystem types, which means we tuned the moss-related parameters for  
240 the six representative ecosystem types. Except for the moss-related parameters, other parameters  
241 related to vascular plants are default based on Zha and Zhuang, 2018. The information of six sites  
242 that we chose to calibrate the TEM\_Moss was compiled in Table 2. The parameterization was  
243 conducted using a global optimization algorithm known as SCE-UA (Shuffled complex evolution)  
244 method, which aims to minimize the difference between model simulations and measurements  
245 (Duan et al., 1994). In our calibration, the cost function of the minimization is:

246 
$$\text{Obj} = \sum_{i=1}^k (\text{NEP}_{\text{obs},i} - \text{NEP}_{\text{sim},i})^2 \quad (19)$$

247 Where  $\text{NEP}_{\text{obs},i}$  and  $\text{NEP}_{\text{sim},i}$  are the measured and simulated NEP, respectively.  $k$  is the number  
248 of data pairs for comparison. Fifty independent sets of parameters were converged to minimize the  
249 objective function, and finally the optimized parameters were derived as the mean of these 50 sets  
250 of inversed parameters. We presented the boxplot of parameter posterior distributions at sites  
251 chosen for calibration (Figure 5). At the same time, the results of model parameterization were

252 shown in Figure 3. Besides these parameters related to moss, all other parameters use their default  
253 values in TEM 5.0 (Zhuang et al., 2003). Note, in TEM 5.0 and its application, the parameters  
254 were also calibrated for each representative ecosystem in northern high latitudes. Specifically,  
255 TEM 5.0 was parameterized for mixed grassland/sub-shrublands, moist non-acidic tundra, mixed  
256 hardwood and conifer forests, tallgrass prairie, savanna tropical forests, tussock tundra, and conifer  
257 forest in the region. TEM 5.0 was then extrapolated to the region to quantify carbon dynamics  
258 without considering the role of moss in boreal ecosystems (Zhuang et al., 2003). Here our revised  
259 model TEM\_Moss was parameterized for representative ecosystems in the region by explicitly  
260 considering the role of moss in soil physics and carbon and nitrogen dynamics. The TEM\_Moss  
261 optimized parameters were then used for model validation and extrapolation as well as comparison  
262 with TEM 5.0 simulations.

263 We verified the TEM\_Moss simulated NEP, soil moisture and soil temperature. First, we  
264 conducted site-level simulations at six sites that contain level-4 gap-filled monthly NEP data from  
265 the AmeriFlux network (Table 3). Site-level monthly gap-filled soil moisture and soil temperature  
266 data were organized from the ORNL DAAC Dataset (<https://daac.ornl.gov/>) to make comparison  
267 with model simulations (Table 4 and Table 5). Local climate data including monthly air  
268 temperature (°C), precipitation (mm), and cloudiness (%) were obtained to drive these model  
269 simulations.

## 270 **2.4 Regional Extrapolation**

271 With six site-level calibrated parameters, TEM-Moss is applied to the region pixel by pixel based  
272 on vegetation distribution data. Both TEM\_Moss and TEM 5.0 were applied to northern high  
273 latitudes (above 45 °N) for historical (the 20<sup>th</sup> century) and future (the 21<sup>st</sup> century) quantifications  
274 on carbon dynamics. For historical simulations, climatic forcing data including monthly air

275 temperature, precipitation, and cloudiness and atmospheric CO<sub>2</sub> concentrations during the 20<sup>th</sup>  
276 century, were collected from the Climatic Research Unit (CRU TS3.1) from the University of East  
277 Anglia (Harris et al., 2014). Other ancillary inputs including gridded soil texture (Zhuang et al.,  
278 2015), elevation (Zhuang et al., 2015), and potential natural vegetation (Melillo et al., 1993) were  
279 also organized. For future simulations, two contrasting Intergovernmental Panel on Climate  
280 Change (IPCC) climate scenarios (RCP 2.6 and RCP 8.5) were used to drive the models. The future  
281 climate forcing data and atmospheric CO<sub>2</sub> concentrations during the 21<sup>st</sup> century under these two  
282 climate change scenarios were derived from the HadGEM2-ESmodel, which is a member of  
283 CMIP5project213 (<https://esgf-node.llnl.gov/search/cmip5/>, January 2017).

284 Simulations were conducted at a spatial resolution of 0.5° latitude × 0.5° longitude (Zhuang  
285 et al., 2001, 2002). A spin-up was run to reach an equilibrium for each pixel, and the values of state  
286 variables at equilibrium were treated as initial values for transient simulations (McGuire et al.,  
287 1992). Specifically, we chose the first 30 years in the whole 100-year climatic forcing data to spin-  
288 up the models when conducting historical and future simulations. For each of the simulations, net  
289 primary production (NPP), heterotrophic respiration (R<sub>H</sub>), and net ecosystem production (NEP)  
290 were analyzed. We denoted that a positive NEP represents a CO<sub>2</sub> sink from the atmosphere to  
291 terrestrial ecosystems, while a negative value represents a source of CO<sub>2</sub> from terrestrial  
292 ecosystems to the atmosphere.

293 In these simulations, for each pixel, we assumed its moss distribution area is the same as  
294 the vascular plant distribution. The total carbon uptake/emission of mosses in a pixel are calculated  
295 as the multiplication of pixel area with the carbon fluxes such as NEP (units: gC m<sup>-2</sup> month<sup>-1</sup>).  
296 Moss-related parameters for representative ecosystems are calibrated (Fig. 4 and Table 1) or

297 obtained from previous model parameterization and the rest of model parameters are default from  
298 Zha and Zhuang (2018).

### 299 **3. Results**

#### 300 **3.1 Model Validation**

301 TEM\_Moss was able to reproduce the monthly NEP and performed better than TEM 5.0  
302 at chosen sites, with larger R-square values and smaller RMSE (Figure 6, Table 6). R-square for  
303 TEM\_Moss reached 0.94 at Bartlett Experimental Forest site and 0.72 at Ivotuk site (Table 6). R-  
304 square values for TEM 5.0 showed a similar pattern, reaching 0.91 and with minimum value of  
305 0.43 at Bartlett Experimental Forest and Ivotuk sites, respectively (Table 6). Except for Ivotuk  
306 site, R-squares for TEM\_Moss are all higher than 0.8 at the chosen sites, while most R-squares  
307 for TEM 5.0 are from 0.62 to 0.75 (Table 6). On the other hand, RMSE for TEM\_Moss is lower  
308 than that for TEM 5.0 at each site (Table 6).

309 We presented the comparisons between measured and simulated volumetric soil moisture  
310 (VSM) from TEM\_Moss and TEM 5.0 (Figure 7). Statistical analysis shows that TEM\_Moss  
311 reproduces the soil moisture well with R-squares ranging from 0.51 at US-Bkg to 0.87 at US-Atq  
312 (Table 7). R-squares for TEM\_Moss are substantially higher than that for TEM 5.0 at most  
313 chosen sites, except for US-Atq (Table 7). RMSE for TEM\_Moss is lower than that for TEM 5.0  
314 at each site (Table 7). Similarly, comparisons between measured and simulated soil temperature  
315 at 5 cm depth (ST\_5) from TEM\_Moss and TEM 5.0 indicated that TEM\_Moss can reproduce  
316 the soil temperature with R-squares ranging from 0.81 at US-Ho1 to 0.91 at US-Bkg, while TEM  
317 5.0 reproduces the soil temperature with R-squares ranging from 0.69 at BE-Vie to 0.89 at US-  
318 Bkg (Figure 8; Table 8). Although R-squares for both models are relatively high and RMSE for

319 them are relatively low, TEM\_Moss still shows higher R-squares and lower RMSE than TEM  
320 5.0 (Table 8).

### 321 **3.2 Regional carbon dynamics during the 20<sup>th</sup> century**

322 Both TEM\_Moss and TEM 5.0 were used to simulate northern high-latitude regional  
323 carbon balance during the 20<sup>th</sup> century (Figure 9). Higher NEP was correlated with the  
324 combination of relatively higher NPP and lower heterotrophic respiration ( $R_H$ ). TEM\_Moss  
325 indicated that the northern high latitudes acted as a carbon sink of 221.9 Pg with an inter-annual  
326 standard deviation of 0.31 PgC yr<sup>-1</sup> during the 20<sup>th</sup> century, which is 132.7 Pg larger than 89.2 Pg  
327 simulated by TEM 5.0 (Figure 10). The simulated NEP by TEM\_Moss ranges from 1.38 PgC yr<sup>-1</sup>  
328 to 3.05 PgC yr<sup>-1</sup>, while the range by TEM 5.0 was from 0.11 PgC yr<sup>-1</sup> to 1.75 PgC yr<sup>-1</sup> (Figure 9).  
329 The patterns of the simulated NEP from two models were similar, both showing a general  
330 increasing trend throughout the 20<sup>th</sup> century (Figure 9). By 2000, the TEM\_Moss simulation  
331 indicated that the northern high-latitude region stored 3.05 PgC yr<sup>-1</sup>, which is more than twice as  
332 the storage estimated by TEM 5.0 (1.33 PgC yr<sup>-1</sup>, Figure 9). Both models indicated that carbon  
333 uptake by the northern ecosystems during the second half of the 20<sup>th</sup> century was higher than the  
334 first half for most part of the region, and only a small portion of the region lost carbon in last  
335 century (Figure 10).

336 Simulated total NPP by TEM\_Moss was 9.6 PgC yr<sup>-1</sup>, ranging from 8.52 PgC yr<sup>-1</sup> to  
337 10.65 PgC yr<sup>-1</sup> in the 20<sup>th</sup> century, with 1.69 PgC yr<sup>-1</sup> of moss NPP and 7.93 PgC yr<sup>-1</sup> of vascular  
338 plants NPP (Figure 9). Moss NPP ranges from 1.23 PgC yr<sup>-1</sup> to 2.14 PgC yr<sup>-1</sup> and the ratio of  
339 moss NPP to vascular plants NPP is 0.21 (Figure 9). TEM 5.0 estimated 0.8 PgC yr<sup>-1</sup> lower total  
340 NPP than TEM\_Moss, but 0.87 PgC yr<sup>-1</sup> higher NPP for vascular plants (Figure 9). On the other  
341 hand, average heterotrophic respiration in the 20<sup>th</sup> century was 7.38 PgC yr<sup>-1</sup> and all years were



342 within about 5% of this value (Figure 9). TEM 5.0 projected 0.53 PgC yr<sup>-1</sup> higher R<sub>H</sub> than  
343 TEM\_Moss (7.91 PgC yr<sup>-1</sup>, Figure 9). Overall, TEM\_Moss predicted higher total NPP but lower  
344 R<sub>H</sub>, which jointly caused a pronounced difference in NEP between two models.

345 Both models estimated that soil organic carbon and vegetation carbon were accumulating  
346 continuously in the 20<sup>th</sup> century (Figure 11). TEM\_Moss indicated that regional SOC and VEGC  
347 accumulated 96.3 PgC and 115.2 PgC, respectively, and the carbon uptake by moss was 10.4 Pg in  
348 the period (Figure 11, Table 10). As simulated by TEM\_Moss, 43.4%, 51.9% and 4.7% of total  
349 carbon uptake in the region was assimilated to soils, vascular plants and mosses, respectively  
350 (Table 10). TEM 5.0 simulated that SOC increased by 31.7 Pg at the end of the 20<sup>th</sup> century,  
351 which is 64.6 PgC less than the value estimated by TEM\_Moss (Table 10). TEM 5.0 estimated  
352 57.7 PgC in plants less than the value estimated by TEM\_Moss (57.5 PgC, Table 10). 35.5% and  
353 64.5% of total carbon was as SOC and VEGC, respectively.

### 354 **3.3 Regional carbon dynamics during the 21<sup>st</sup> century**

355 Under the RCP 2.6 scenario, TEM\_Moss simulated NEP of 2.07 PgC yr<sup>-1</sup> with the range  
356 from 0.41 PgC yr<sup>-1</sup> to 3.2 PgC yr<sup>-1</sup>, and the inter-annual standard deviation of 0.59 PgC yr<sup>-1</sup>  
357 during the 21<sup>st</sup> century (Figure 12 (a)). The regional sink shows a decreasing pattern in the 2000s  
358 and then generally increases over the remaining years of the 21<sup>st</sup> century (Figure 12 (a)). For  
359 comparison, TEM 5.0 predicted that the average NEP of 0.28 PgC yr<sup>-1</sup> with the range from -1.48  
360 PgC yr<sup>-1</sup> to 1.69 PgC yr<sup>-1</sup> during the 21<sup>st</sup> century (Figure 12 (a)). Thus, TEM 5.0 projected 179.1  
361 PgC stored in northern ecosystems is less than the estimation from TEM\_Moss in the 21<sup>st</sup>  
362 century. Besides, TEM 5.0 simulated that the regional NEP showed a decreasing trend and the  
363 region fluctuates between sinks and sources during the century (Figure 12 (a)). The spatial  
364 patterns from two models also showed differences. TEM\_Moss indicated that the region

365 accumulates carbon over this century, while TEM 5.0 simulated that some regions changed from  
366 a carbon sink to a source in the second half of the century (Figure 13 (a)). Simulated regional  
367 NPP by TEM\_Moss ranges from 11.2 to 13.7 PgC yr<sup>-1</sup> with a mean of 12.98 PgC yr<sup>-1</sup> in this  
368 century, while average NPP predicted by TEM 5.0 is 1.46 PgC yr<sup>-1</sup> lower than that value (11.52  
369 PgC yr<sup>-1</sup> (Figure 12(a)). TEM\_Moss simulated NPP has 3.74 PgC yr<sup>-1</sup> from moss and 9.24 PgC  
370 yr<sup>-1</sup> from vascular plants, which account for 28.8% and 71.2% of total NPP, respectively (Figure  
371 12(a)). Meanwhile, TEM\_Moss estimated that R<sub>H</sub> is 10.91 PgC yr<sup>-1</sup>, while TEM 5.0 predicted it  
372 as 11.24 PgC yr<sup>-1</sup>, which is higher (Figure 12(b)). Both models projected that soil organic carbon  
373 and vegetation carbon accumulate in this century but with different magnitudes (Figure 14 (a)).  
374 TEM\_Moss predicted that regional SOC and VEGC accumulated 84.7 PgC and 112.6 PgC,  
375 respectively, during the 21<sup>st</sup> century, while TEM 5.0 predicted that a smaller increase with 12.1  
376 and 15.5 PgC in SOC and VEGC, respectively (Figure 14 (a), Table 12 (a)). Besides, TEM\_Moss  
377 also predicted an increasing of 9.4 PgC in MOSSC, accounting for 4.5% of the total carbon  
378 uptake in this region (Table 12(a)).

379 Under the RCP 8.5 scenario, TEM\_Moss simulated annual NPP of 13.84 PgC yr<sup>-1</sup> with a  
380 range from 11.09 to 16.94 PgC yr<sup>-1</sup>, which is 1.31 PgC yr<sup>-1</sup> higher than the projection from TEM  
381 5.0 (Figure 12 (b)). Total NPP estimated by TEM\_Moss has 3.84 PgC yr<sup>-1</sup> from moss and 10  
382 PgC yr<sup>-1</sup> from vascular plants (Figure 12(b)). Annual R<sub>H</sub> was 11.28 PgC yr<sup>-1</sup> estimated by  
383 TEM\_Moss and 11.54 PgC yr<sup>-1</sup> by TEM 5.0, respectively (Figure 12(b)). Consequently,  
384 TEM\_Moss projected NEP was 2.56 PgC yr<sup>-1</sup> with the inter-annual standard deviation of 0.93  
385 PgC yr<sup>-1</sup> in this century (Figure 12(b)). NEP ranges from 0.67 PgC yr<sup>-1</sup> to 4.78 PgC yr<sup>-1</sup>  
386 estimated with TEM\_Moss, while from -1.69 PgC yr<sup>-1</sup> to 2.65 PgC yr<sup>-1</sup> with a mean of 0.99 PgC  
387 yr<sup>-1</sup> was estimated by TEM 5.0 (Figure 12(b)). TEM\_Moss predicted more carbon uptake of

388 157.5 Pg than TEM 5.0 during the 21<sup>st</sup> century. Both models predicted that NEP showed an  
389 increasing trend during the 21<sup>st</sup> century (Figure 12(b)). Moreover, similar spatial patterns of  
390 carbon sinks and sources appeared in the projections from two models (Figure 13(b)). Soil  
391 organic carbon and vegetation carbon shows an increasing trend from both models (Figure  
392 14(b)). Regional SOC and VEGC increased by 92.5 PgC and 153.6 PgC, respectively by the end  
393 of the 21<sup>st</sup> century predicted by TEM\_Moss. In contrast, the increase of 44.2 PgC and 54.5 PgC of  
394 SOC and VEGC, respectively, was predicted by TEM 5.0 (Figure 14(b), Table 12 (b)). TEM\_Moss  
395 predicted an increase of 10.1 PgC in MOSSC (Table 12(b)).

## 396 **4. Discussion**

### 397 **4.1 The role of moss in the regional carbon dynamics**

398  
399 Global warming has been pronounced in recent decades, particularly at high latitudes  
400 (IPCC, 2014; Tape et al., 2006; Stow et al., 2004). An enormous amount of soil organic carbon  
401 stored in northern high-latitude regions (Tarnocai et al., 2009; Schuur et al., 2008) is expected to  
402 affect a broad spectrum of ecological and human systems, and cause rapid changes in the Earth  
403 system when undergoing substantial climate change (Serreze and Francis 2006; Davidson and  
404 Janssens, 2006; McGuire et al., 2009). Improving projections for carbon budget of high latitude  
405 terrestrial ecosystems is essential for understanding global carbon–climate feedbacks (Melillo et  
406 al., 2011; Todd-Brown et al., 2013).

407 Our simulations suggest that mosses play an important role in the regional carbon  
408 dynamics, which is consistent with previous studies (McGuire et al., 2009; Turetsky et al., 2012).  
409 First of all, mosses are productive with carbon assimilation even during low temperature, water  
410 content and irradiance (Kallio and Heinonen, 1975; Harley et al., 1989). For example, mosses  
411 can tolerate drought through physiological responses, such as by suspending metabolism and by

412 withstanding cell desiccation (Turetsky et al., 2012; Oechel and Van Cleve, 1986). The key  
413 functional traits related to water, nutrient, and thermal tolerances of mosses enable them to fit in  
414 harsh northern conditions (Shetler et al., 2008; Turetsky et al., 2012). Thus, with incorporation of  
415 moss into our models, the total NPP estimation in our model is affected. Mosses also act as a  
416 powerful competitor with vascular plants for nutrient uptake. Their rapid nutrient acquisition and  
417 slow nutrient loss through slow decomposition may constrain concentrations of plant-available  
418 nitrogen (Hobbie et al., 2000; Turetsky et al., 2010; Oechel and Van Cleve, 1986; Gornall et al.,  
419 2007), which will further decrease NPP of vascular plants. Our model results suggested that the  
420 NPP of vascular plants considering moss is indeed lower than previous NPP estimates without  
421 considering moss, but the total NPP is larger than before. We estimated that mosses contribute  
422 17.6% of NPP in the 20<sup>th</sup> century, and 28.8% and 27.6% in the 21<sup>st</sup> century under the RCP 2.6  
423 and RCP 8.5 scenarios, respectively. This is comparable with the results reported by a synthesis  
424 study, indicating an average contribution 20% of aboveground NPP from moss in upland boreal  
425 forests and the contribution is 48% in wetlands ecosystems. Frohking et al. (1996) even reported  
426 a contribution of 38.4% to total NPP by moss at a boreal forest site. Moreover, mosses can also  
427 influence heterotrophic respiration ( $R_H$ ) through their effects on soil thermal and hydrologic  
428 dynamics (Zhuang et al., 2001). With the layer of moss, soil temperature tends to decrease but  
429 soil moisture tends to increase (Oechel and Van Cleve, 1986), which will further decrease soil  
430 respiration in summer. This supports our results that TEM\_Moss simulated  $R_H$  is lower than that  
431 by TEM 5.0. With a combination of higher NPP and lower  $R_H$ , NEP predicted by TEM\_Moss is  
432 larger than that by TEM 5.0. The two contrasting regional simulations by TEM\_Moss and TEM  
433 5.0 indicated the region is currently a carbon sink, which is consistent with previous studies  
434 (White et al., 2000; McGuire et al., 2009; Schimel et al., 2001). Our study estimates that regional

435 NEP during the 20<sup>th</sup> century is 2.2 Pg C yr<sup>-1</sup> by TEM\_Moss and 0.89 Pg C yr<sup>-1</sup> by TEM 5.0,  
436 respectively. In the 1990s, the regional sink is projected to be 2.7 and 1.1 Pg C yr<sup>-1</sup> by  
437 TEM\_Moss and TEM 5.0 respectively. Compared with other existing studies, our regional  
438 estimates of NEP are within the reasonable range from other existing studies. McGuire et al.  
439 (2009) estimated a land sink of 0.3–0.6 Pg C yr<sup>-1</sup> for the pan-arctic region for the 1990s, which is  
440 closer to our estimation by TEM 5.0 but less than the projection by TEM\_Moss. The top-down  
441 atmospheric analyses indicate that the sink of pan-arctic region is between 0 and 0.8 Pg C yr<sup>-1</sup> in  
442 the 1990s (Menon et al. 2007). Besides, Schimel et al. (2001) reported an estimation of the  
443 northern extratropical NEP is from 0.6 to 2.3 PgC yr<sup>-1</sup> in the late 20<sup>th</sup> century, which is  
444 comparable to our estimates. Our simulations also confirmed that mosses and vascular plants  
445 respond to climate change similarly in terms of their productivity (Turetsky et al. 2010).

#### 446 **4.2 Model Uncertainty and limitations**

447       There are a number of uncertainty sources in our model simulations. First, due to the  
448 limited understanding of moss photosynthesis (He et al., 2015) and various moss N uptake  
449 pathways (e.g., Bay et al 2013; Berg et al 2013), a few important assumptions have been made in  
450 our modeling. For instance, we assume that mosses behave similarly to vascular plants regarding  
451 photosynthesis and soil N uptake is the only pathway for mosses without considering N uptake  
452 through N fixers and atmospheric wet N deposition (Ayres et al. 2006). Second, the errors in the  
453 observed data will influence our parameterization results, which will bias our regional estimates  
454 of carbon dynamics. Second, climatic driving data are also a source of uncertainty for historical  
455 and future simulations. Third, model assumptions will also induce additional uncertainties. For  
456 instance, we assumed that vegetation distribution will remain unchanged during the transient  
457 simulation. However, vegetation will change in response to warming climate and disturbances

458 such as fire and insect outbreaks in the region (Hansen et al., 2006), which will affect carbon  
459 budget. Missing potential responses to disturbances in our model shall introduce additional  
460 uncertainties (Soja et al. 2007; Kasischke and Turetsky, 2006). Future moss dynamics will also  
461 impact carbon dynamics in this region. For instance, a long-term warming experiments along  
462 natural climatic gradients, ranging from Swedish subarctic birch forest and subarctic/subalpine  
463 tundra to Alaskan arctic tussock tundra concluded that both diversity and abundance of mosses  
464 are likely to decrease under arctic climate warming (Long et al. 2012). Similarly, total moss  
465 cover declined in both heath and mesic meadow under experimental long-term warming (by 1.5–  
466 3 °C), driven by general declines in many species (Alatalo et al., 2020). Due to global warming,  
467 significant losses in moss diversity are expected in boreal forests and alpine biomes, leading to  
468 changes in ecosystem structure and function, nutrient cycling, and carbon balance (He et al.,  
469 2015).

470 We conducted ensemble regional simulations with 50 sets of parameters to quantify  
471 model uncertainty due to uncertain parameters. The 50 sets of parameters were obtained using  
472 the method in Tang and Zhuang (2008). The ensemble means and the inter-simulation standard  
473 deviations are used to measure the model uncertainty (Figure 15). TEM\_Moss predicted that the  
474 regional cumulative carbon ranges from a carbon loss of 266 Pg C to a carbon sink of 567.3 Pg C  
475 by different ensemble members, with a mean of  $161.1 \pm 142.1$  Pg during the 21<sup>st</sup> century under the  
476 RCP 2.6 scenario. Under the RCP 8.5 scenario, TEM\_Moss predicted that the region acts from a  
477 carbon source of 79.1 Pg C to a carbon sink of 625.9 Pg C, with a mean of  $186.7 \pm 166.1$  Pg  
478 during the 21<sup>st</sup> century (Figure 15).

479 This study took an important step to incorporate moss into an extant ecosystem model  
480 that has not explicitly consider the role of moss and its interactions with vascular plants. Our

481 model simulations showed that mosses have strong influences on regional ecosystem carbon  
482 cycling, by affecting the soil thermal, nitrogen availability, and water conditions of terrestrial  
483 ecosystems. However, there are still limitations in our model. First, we did not differentiate  
484 various kinds of mosses because they have their own functional traits. Different kinds of mosses  
485 may provide different levels of insulation for soil, resulting in different soil thermal conditions  
486 that affect microbial activities. The structural and physiological traits of mosses will differ  
487 largely in different moss groups, such as feather moss versus Sphagnum (Turetsky et al., 2010).  
488 In addition, we lack spatially explicit information of moss distribution in the region, which will  
489 lead to a large regional uncertainty of carbon quantification. We assumed that moss area  
490 distribution is the same as its associated vegetation distribution. Another limitation is that some  
491 important physiological traits of moss have not been modeled. For example, moss abundance  
492 may change following shifts in vascular species composition due to shading or burial by vascular  
493 litter (Turetsky et al., 2010; Cornelissen et al., 2007). Furthermore, disturbance such as wildfires  
494 can also influence moss activities.

## 495 **5. Conclusions**

496 This study explicitly incorporated moss into an extant process-based terrestrial ecosystem model  
497 to investigate the carbon dynamics in the Arctic for present day and future. Historical regional  
498 simulations with TEM\_Moss indicated that the region is a carbon sink of 221.9 PgC over the 20<sup>th</sup>  
499 century, and this sink may decrease to 206.7 PgC under the RCP 2.6 scenario or increase to 256.2  
500 PgC under the RCP 8.5 scenario during the 21<sup>st</sup> century. Compared with an earlier version of TEM  
501 that has not explicitly modeled moss, TEM\_Moss projected that the region stored 132.7 Pg more  
502 C over the last century, 179.1 Pg and 157.5 Pg more C under the RCP 2.6 and RCP 8.5 scenarios,  
503 respectively. This study demonstrated that moss activities have large effects on ecosystem soil

504 thermal, water, and carbon dynamics through their interactions with vascular plants. This study  
505 highlights the importance of considering the moss dynamics in Earth System Models to adequately  
506 quantify the carbon–climate feedbacks in the Arctic.

## 507 **6. Acknowledgments**

508 This research was supported by an NSF project (IIS-1027955), a DOE project (DE-SC0008092),  
509 and a NASA LCLUC project (NNX09AI26G). We acknowledge the Rosen High Performance  
510 Computing Center at Purdue for computing support. We also acknowledge the World Climate  
511 Research Programme’s Working Group on Coupled Modeling Intercomparison Project CMIP5,  
512 and we thank the climate modeling groups for producing and making available their model  
513 output. The data of this study can be accessed from Purdue Research Repository.

514

## 515 **References**

- 516 Allison, S. D., and Treseder, K. K.: Warming and drying suppress microbial activity and carbon cycling in  
517 boreal forest soils, *Global change biology*, 14, 2898-2909, 10.1111/j.1365-2486.2008.01716.x, 2008.
- 518 Basilier, K.: Moss-associated nitrogen fixation in some mire and coniferous forest environments around  
519 Uppsala, Sweden, *Lindbergia*, 5, 84-88, 1979.
- 520 Bay, G., Nahar, N., Oubre, M., Whitehouse, M.J., Wardle, D.A., Zackrisson, O., Nilsson, M.-C. and  
521 Rasmussen, U. (2013), Boreal feather mosses secrete chemical signals to gain nitrogen. *New Phytol*, 200:  
522 54-60. <https://doi.org/10.1111/nph.12403>
- 523 Ben Bond-Lamberty, S. T. G., Douglas E. Ahl and Peter E. Thornton: Reimplementation of the Biome-  
524 BGC model to simulate successional change, *Tree Physiology*, 25, 413–424, 2005.
- 525 Berg, Andreas, et al. “Transfer of Fixed-N from N<sub>2</sub>-Fixing Cyanobacteria Associated with the Moss  
526 *Sphagnum Riparium* Results in Enhanced Growth of the Moss.” *Plant and Soil*, vol. 362, no. 1/2, 2013,  
527 pp. 271–278. JSTOR, [www.jstor.org/stable/42951898](http://www.jstor.org/stable/42951898). Accessed 28 May 2021.
- 528 Bond-Lamberty, B., Peckham, S. D., Ahl, D. E., and Gower, S. T.: Fire as the dominant driver of central  
529 Canadian boreal forest carbon balance, *Nature*, 450, 89-92, 10.1038/nature06272, 2007.
- 530 Bond-Lamberty, B., and Thomson, A.: Temperature-associated increases in the global soil respiration  
531 record, *Nature*, 464, 579-582, 10.1038/nature08930, 2010.



532 Burke, E. J., Ekici, A., Huang, Y., Chadburn, S. E., Huntingford, C., Ciais, P., Friedlingstein, P., Peng, S.  
533 & Krinner, G. 2017. Quantifying uncertainties of permafrost carbon-climate feedbacks. *Biogeosciences*,  
534 14, 3051-3066.

535 Cahoon, S. M., Sullivan, P. F., Shaver, G. R., Welker, J. M., Post, E., and Holyoak, M.: Interactions  
536 among shrub cover and the soil microclimate may determine future Arctic carbon budgets, *Ecology*  
537 letters, 15, 1415-1422, 10.1111/j.1461-0248.2012.01865.x, 2012.

538 Chadburn, S. E., Burke, E. J., Cox, P. M., Friedlingstein, P., Hugelius, G., and Westermann, S.: An  
539 observation-based constraint on permafrost loss as a function of global warming, *Nature Climate Change*,  
540 7, 340-344, 10.1038/nclimate3262, 2017.

541 Charles J. Vörösmarty, B. M. I., Annette L. Grace, and M. Patricia Gildea: Continental scale models of  
542 water balance and fluvial transport: an application to South America, *Global biogeochemical cycles*, 3,  
543 241-265, 1989.

544 Christian Fritz, L. P. M. L., Muhammad Riaz, Leon J. L. van den Berg, Theo J. T.M. Elzenga: Sphagnum  
545 Mosses - Masters of Efficient N-Uptake while Avoiding Intoxication, *PLoS ONE*, 9,  
546 10.1371/journal.pone.0079991, 2014.

547 Clarke, G. C. S.: Productivity of Bryophytes in Polar Regions, *Annals of botany*, 35, 99–108, 1971.

548 Collins, W. C. O. a. N. J.: Comparative CO<sub>2</sub> exchange patterns in mosses from two tundra habitats at  
549 Barrow, Alaska, *Canadian Journal of Botany*, 54, 1355-1369, 1976.

550 Comyn-Platt, E., Hayman, G., Huntingford, C., Chadburn, S. E., Burke, E. J., Harper, A. B., Collins, W.  
551 J., Webber, C. P., Powell, T., Cox, P. M., Gedney, N. & Sitch, S. 2018. Carbon budgets for 1.5 and 2 °C  
552 targets lowered by natural wetland and permafrost feedbacks. *Nature Geoscience*, 11, 568-573.

553 Cornelissen, J. H., Lang, S. I., Soudzilovskaia, N. A., and During, H. J.: Comparative cryptogam ecology:  
554 a review of bryophyte and lichen traits that drive biogeochemistry, *Annals of botany*, 99, 987-1001,  
555 10.1093/aob/mcm030, 2007.

556 Davidson, E. A., Trumbore, S. E., and Amundson, R.: Soil warming and organic carbon content, *Nature*,  
557 408, 789, 10.1038/35048672, 2000.

558 Davidson, E. A., and Janssens, I. A.: Temperature sensitivity of soil carbon decomposition and feedbacks  
559 to climate change, *Nature*, 440, 165-173, 10.1038/nature04514, 2006.

560 Davidson, E. A., Janssens, I. A., and Luo, Y.: On the variability of respiration in terrestrial ecosystems:  
561 moving beyond Q<sub>10</sub>, *Global change biology*, 12, 154-164, 10.1111/j.1365-2486.2005.01065.x, 2006.

562 DeLuca, T. H., Zackrisson, O., Gentili, F., Sellstedt, A., and Nilsson, M. C.: Ecosystem controls on  
563 nitrogen fixation in boreal feather moss communities, *Oecologia*, 152, 121-130, 10.1007/s00442-006-  
564 0626-6, 2007.

565 Duan, Q., Sorooshian, S., and Gupta, V. K.: Optimal use of the SCE-UA global optimization method for  
566 calibrating watershed models, *Journal of Hydrology*, 158, 265-284, 1994.

567 E. S. Euskirchen, A. D. M., F. S. Chapin, III, S. Yi, and C. C. Thompson: Changes in vegetation in  
568 northern Alaska under scenarios of climate change, 2003–2100: implications for climate feedbacks,  
569 *Ecological Applications*, 19, 1022–1043, 2009.

570 Edward A. G. Schuur, J. B., Josep G. Canadell, Eugenie Euskirchen, Christopher B., Field, S. V. G.,  
571 Stefan Hagemann, Peter Kuhry, Peter M. Lafleur, Hanna Lee, Galina, Mazhitova, F. E. N., Annette Rinke,  
572 Vladimir E. Romanovsky, Nikolay Shiklomanov, and Charles Tarnocai, S. V., Jason G. Vogel, And Sergei  
573 A. Zimov: Vulnerability of Permafrost Carbon to Climate Change: Implications for the Global Carbon  
574 Cycle, *BioScience*, 58, 701-714, 2008.

575 Edward Ayres, R. v. d. W., Martin Sommerkorn, Richard D. Bardgett: Direct uptake of soil nitrogen by  
576 mosses, *Biology Letters*, 2, 286-288, 10.1098/rsbl.2006.0455, 2006.

577 Esteban G. Jobbágy, and Jackson, R. B.: The vertical distribution of soil organic carbon and its relation to  
578 climate and vegetation, *Ecological applications*, 10, 423-436, 2000.

579 Frolking, S., Roulet, N. T., Tuittila, E., Bubier, J. L., Quillet, A., Talbot, J., and Richard, P. J. H.: A new  
580 model of Holocene peatland net primary production, decomposition, water balance, and peat  
581 accumulation, *Earth System Dynamics*, 1, 1-21, 10.5194/esd-1-1-2010, 2010.

582 Gilmanov, T. G., Tieszen, L. L., Wylie, B. K., Flanagan, L. B., Frank, A. B., Haferkamp, M. R., Meyers,  
583 T. P., and Morgan, J. A.: Integration of CO<sub>2</sub> flux and remotely-sensed data for primary production and  
584 ecosystem respiration analyses in the Northern Great Plains: potential for quantitative spatial  
585 extrapolation, *Global Ecology and Biogeography*, 14, 271-292, 10.1111/j.1466-822X.2005.00151.x, 2005.

586 Gornall, J. L., Jonsdottir, I. S., Woodin, S. J., and Van der Wal, R.: Arctic mosses govern below-ground  
587 environment and ecosystem processes, *Oecologia*, 153, 931-941, 10.1007/s00442-007-0785-0, 2007.

588 Gornall, J. L., Woodin, S. J., Jonsdottir, I. S., and van der Wal, R.: Balancing positive and negative plant  
589 interactions: how mosses structure vascular plant communities, *Oecologia*, 166, 769-782,  
590 10.1007/s00442-011-1911-6, 2011.

591 Gough, C. M., Hardiman, B. S., Nave, L. E., Bohrer, G., Maurer, K. D., Vogel, C. S., Nadelhoffer, K. J.,  
592 and Curtis, P. S.: Sustained carbon uptake and storage following moderate disturbance in a Great Lakes  
593 forest, *Ecological Applications*, 23, 1202-1215, 2013.

594 Goulden, M. L., Winston, G. C., McMillan, A. M. S., Litvak, M. E., Read, E. L., Rocha, A. V., and Rob  
595 Elliot, J.: An eddy covariance mesonet to measure the effect of forest age on land atmosphere exchange,  
596 *Global change biology*, 12, 2146-2162, 10.1111/j.1365-2486.2006.01251.x, 2006.

597 Hansen, J., Sato, M., Ruedy, R., Lo, K., Lea, D. W., and Medina-Elizade, M.: Global temperature change,  
598 Proceedings of the National Academy of Sciences of the United States of America, 103, 14288-14293,  
599 10.1073/pnas.0606291103, 2006.

600 Harris, I., Jones, P. D., Osborn, T. J., and Lister, D. H.: Updated high-resolution grids of monthly climatic  
601 observations - the CRU TS3.10 Dataset, International Journal of Climatology, 34, 623-642,  
602 10.1002/joc.3711, 2014.

603 Hayes, D. J., McGuire, A. D., Kicklighter, D. W., Gurney, K. R., Burnside, T. J., and Melillo, J. M.: Is the  
604 northern high-latitude land-based CO<sub>2</sub> sink weakening?, Global Biogeochemical Cycles, 25, n/a-n/a,  
605 10.1029/2010gb003813, 2011.

606 Hayes, D. J., Kicklighter, D. W., McGuire, A. D., Chen, M., Zhuang, Q., Yuan, F., Melillo, J. M., and  
607 Wullschleger, S. D.: The impacts of recent permafrost thaw on land-atmosphere greenhouse gas  
608 exchange, Environmental Research Letters, 9, 045005, 10.1088/1748-9326/9/4/045005, 2014.

609 Xiaolan He, Kate S. He, Jaakko Hyvönen, Will bryophytes survive in a warming world?,  
610 Perspectives in Plant Ecology, Evolution and Systematics, Volume 19, 2016, Pages 49-60,  
611 ISSN 1433-8319, <https://doi.org/10.1016/j.ppees.2016.02.005>.

612 Hiller, R. V., McFadden, J. P., and Kljun, N.: Interpreting CO<sub>2</sub> Fluxes Over a Suburban Lawn: The  
613 Influence of Traffic Emissions, Boundary-Layer Meteorology, 138, 215-230, 10.1007/s10546-010-9558-  
614 0, 2010.

615 Hugelius, G., Strauss, J., Zubrzycki, S., Harden, J. W., Schuur, E. A. G., Ping, C. L., Schirmer, L.,  
616 Grosse, G., Michaelson, G. J., Koven, C. D., amp, apos, Donnell, J. A., Elberling, B., Mishra, U., Camill,  
617 P., Yu, Z., Palmtag, J., and Kuhry, P.: Estimated stocks of circumpolar permafrost carbon with quantified  
618 uncertainty ranges and identified data gaps, Biogeosciences, 11, 6573-6593, 10.5194/bg-11-6573-2014,  
619 2014.

620 Jägerbrand, A. K., Lindblad, K. E. M., Björk, R. G., Alatalo, J. M., and Molau, U.: Bryophyte and Lichen  
621 Diversity Under Simulated Environmental Change Compared with Observed Variation in Unmanipulated  
622 Alpine Tundra, Biodiversity and Conservation, 15, 4453-4475, 10.1007/s10531-005-5098-1, 2006.

623 Jenkins, J. P., Richardson, A. D., Braswell, B. H., Ollinger, S. V., Hollinger, D. Y., and Smith, M. L.:  
624 Refining light-use efficiency calculations for a deciduous forest canopy using simultaneous tower-based  
625 carbon flux and radiometric measurements, Agricultural and Forest Meteorology, 143, 64-79,  
626 10.1016/j.agrformet.2006.11.008, 2007.

627 Juha M Alatalo, Annika K Jägerbrand, Mohammad Bagher Erfanian, Shengbin Chen, Shou-Qin Sun, Ulf  
628 Molau, Bryophyte cover and richness decline after 18 years of experimental warming in alpine Sweden,  
629 AoB PLANTS, Volume 12, Issue 6, December 2020, plaa061, <https://doi.org/10.1093/aobpla/plaa061>

630 Kasischke, E. S.: Boreal ecosystems in the global carbon cycle. In Fire, climate change, and carbon  
631 cycling in the boreal forest, *Ecological Studies (Analysis and Synthesis)*, 138, 19-30,  
632 [https://doi.org/10.1007/978-0-387-21629-4\\_2](https://doi.org/10.1007/978-0-387-21629-4_2), 2000.

633 Kasischke, E. S., and Turetsky, M. R.: Recent changes in the fire regime across the North American  
634 boreal region—Spatial and temporal patterns of burning across Canada and Alaska, *Geophysical Research*  
635 *Letters*, 33, 10.1029/2006gl025677, 2006.

636 Kip, N., Ouyang, W., van Winden, J., Raghoebarsing, A., van Niftrik, L., Pol, A., Pan, Y., Bodrossy, L.,  
637 van Donselaar, E. G., Reichart, G. J., Jetten, M. S., Damste, J. S., and Op den Camp, H. J.: Detection,  
638 isolation, and characterization of acidophilic methanotrophs from Sphagnum mosses, *Applied and*  
639 *environmental microbiology*, 77, 5643-5654, 10.1128/AEM.05017-11, 2011.

640 Knorr, W.: Annual and interannual CO<sub>2</sub> exchanges of the terrestrial biosphere: process-based simulations  
641 and uncertainties, *Global Ecology and Biogeography*, 9, 225-252, 2000.

642 Koven, C. D., Schuur, E. A. G., Schädel, C., Bohn, T. J., Burke, E. J., Chen, G., Chen, X., Ciais, P.,  
643 Grosse, G., Harden, J. W., Hayes, D. J., Hugelius, G., Jafarov, E. E., Krinner, G., Kuhry, P., Lawrence, D.  
644 M., Macdougall, A. H., Marchenko, S. S., Mcguire, A. D., Natali, S. M., Nicolsky, D. J., Olefeldt, D.,  
645 Peng, S., Romanovsky, V. E., Schaefer, K. M., Strauss, J., Treat, C. C. & Turetsky, M. 2015. A simplified,  
646 data-constrained approach to estimate the permafrost carbon-climate feedback. *Philosophical*  
647 *Transactions of the Royal Society A: Mathematical, Physical and Engineering Sciences*, 373.

648 L. Kulmala, J. P., P. Hari and T. Vesala: Photosynthesis of ground vegetation in different aged pine forests:  
649 Effect of environmental factors predicted with a process-based model, *Journal of Vegetation Science*, 22,  
650 96–110, 2011.

651 Launiainen, S., Katul, G. G., Lauren, A., and Kolari, P.: Coupling boreal forest CO<sub>2</sub>, H<sub>2</sub>O and energy  
652 flows by a vertically structured forest canopy – Soil model with separate bryophyte layer, *Ecological*  
653 *Modelling*, 312, 385-405, 10.1016/j.ecolmodel.2015.06.007, 2015.

654 Lindo, Z., and Gonzalez, A.: The Bryosphere: An Integral and Influential Component of the Earth's  
655 Biosphere, *Ecosystems*, 13, 612-627, 10.1007/s10021-010-9336-3, 2010.

656 Lang, S.I., Cornelissen, J.H.C., Shaver, G.R., Ahrens, M., Callaghan, T.V., Molau, U., Ter Braak, C.J.F.,  
657 Hölzer, A. and Aerts, R. (2012), Arctic warming on two continents has consistent negative effects on  
658 lichen diversity and mixed effects on bryophyte diversity. *Glob Change Biol*, 18: 1096-1107.  
659 <https://doi.org/10.1111/j.1365-2486.2011.02570.x>

660 Longton, R. E.: Adaptations and strategies of polar bryophytes, *Botanical Journal of the Linnean Society*,  
661 98, 253-268, 1988.

662 Markham, J. H.: Variation in moss-associated nitrogen fixation in boreal forest stands, *Oecologia*, 161,  
663 353-359, 10.1007/s00442-009-1391-0, 2009.

664 McEwing, K. R., Fisher, J. P., and Zona, D.: Environmental and vegetation controls on the spatial  
665 variability of CH<sub>4</sub> emission from wet-sedge and tussock tundra ecosystems in the Arctic, *Plant and soil*,  
666 388, 37-52, 10.1007/s11104-014-2377-1, 2015.

667 McGuire, A. D., Melillo, J. M., Joyce, L. A., Kicklighter, D. W., Grace, A. L., III, B. M., and Vorosmarty,  
668 C. J.: Interactions between carbon and nitrogen dynamics in estimating net primary productivity for  
669 potential vegetation in North America, *Global Biogeochemical Cycles*, 6, 101-124, 1992.

670 McGuire, A. D., Melillo, J. M., Kicklighter, D. W., and Joyce, L. A.: Equilibrium responses of soil carbon  
671 to climate change: Empirical and process-based estimates, *Journal of Biogeography*, 785-796, 1995.

672 McGuire, A. D., and Hobbie, J. E.: Global climate change and the equilibrium responses of carbon  
673 storage in arctic and subarctic regions, In *Modeling the Arctic system: A workshop report on the state of*  
674 *modeling in the Arctic System Science program*, 53-54, 1997.

675 McGuire, A. D., Anderson, L. G., Christensen, T. R., Dallimore, S., Guo, L., Hayes, D. J., Heimann, M.,  
676 Lorenson, T. D., Macdonald, R. W., and Roulet, N.: Sensitivity of the carbon cycle in the Arctic to climate  
677 change, *Ecological Monographs*, 79, 523-555, 2009.

678 Melillo, J. M., McGuire, A. D., Kicklighter, D. W., Moore, B., Vorosmarty, C. J., and Schloss, A. L.:  
679 Global climate change and terrestrial net primary production, *Nature*, 363, 234, 10.1038/363234a0, 1993.

680 Melillo, J. M., Butler, S., Johnson, J., Mohan, J., Steudler, P., Lux, H., Burrows, E., Bowles, F., Smith, R.,  
681 Scott, L., Vario, C., Hill, T., Burton, A., Zhou, Y.-M., and Tang, J.: Soil warming, carbon - nitrogen  
682 interactions, and forest carbon budgets, *PNAS*, 108, 9508-9512, 2011.

683 Naomi Oreskes, K. S.-F., Kenneth Belitz: Verification, validation, and confirmation of numerical models  
684 in the earth sciences, *Science*, 263, 641-646, 1994.

685 O. Skre, W. C. O.: Moss production in a black spruce *Picea mariana* forest with permafrost near  
686 Fairbanks, Alaska, as compared with two permafrost-free stands, *Ecography*, 2, 249-254, 1979.

687 Oechel, W. C., Laskowski, C. A., Burba, G., Gioli, B., and Kalhori, A. A. M.: Annual patterns and budget  
688 of CO<sub>2</sub> flux in an Arctic tussock tundra ecosystem, *Journal of Geophysical Research: Biogeosciences*,  
689 119, 323-339, 10.1002/2013jg002431, 2014.

690 Okland, R. H.: Population Biology of the Clonal Moss *Hylocomium Splendens* in Norwegian Boreal  
691 Spruce Forests. I. Demography, *Journal of Ecology*, 83, 697-712, 1995.

692 P.C. Harley, J. D. T., K.J. Murray, and J. Beyers: Irradiance and temperature effects on photosynthesis of  
693 tussock tundra *Sphagnum* mosses from the foothills of the Philip Smith Mountains, Alaska, *Oecologia*,  
694 79, 251-259, 1989.

695 Pakarinen, P., and D. H. Vitt: Primary production of plant communities of the Truelove Lowland, Devon  
696 Island, Canada—Moss communities, Primary production and production processes, tundra biome.  
697 International Biological Programme, Tundra Biome Steering Committee, Edmonton Oslo, 37-46, 1973.

698 Pharo, E. J., and Zartman, C. E.: Bryophytes in a changing landscape: The hierarchical effects of habitat  
699 fragmentation on ecological and evolutionary processes, *Biological Conservation*, 135, 315-325,  
700 10.1016/j.biocon.2006.10.016, 2007.

701 Raich, J. W., Rastetter, E. B., Melillo, J. M., Kicklighter, D. W., Steudler, P. A., Peterson, B. J., Grace, A.  
702 L., III, B. M., and Vorosmarty, C. J.: Potential net primary productivity in South America: application of a  
703 global model, *Ecological Applications*, 1, 399-429, 1991.

704 Richardson, A. D., Jenkins, J. P., Braswell, B. H., Hollinger, D. Y., Ollinger, S. V., and Smith, M. L.: Use  
705 of digital webcam images to track spring green-up in a deciduous broadleaf forest, *Oecologia*, 152, 323-  
706 334, 10.1007/s00442-006-0657-z, 2007.

707 Running, S. W., and Coughlan, J. C.: A general model of forest ecosystem processes for regional  
708 applications I. Hydrologic balance, canopy gas exchange and primary production processes., *Ecological*  
709 *Modelling*, 42, 125-154, 1988.

710 S. Frohking, M. L. G., S.C. Wofsy, S-M. Fan, D.J. Sutton, J.W. Munger, A.M. Bazzaz, B.C. Daube, P.M.  
711 Crill, J.D, Aber, L.E. Band, X. Wang, K. Savage, T. Moore and R.C. Harriss: Modelling temporal  
712 variability in the carbon balance of a spruce/moss boreal forest, *Global change biology*, 2, 343-366, 1996.

713 Sarah E. Hobbie, J. P. S., Susan E. Trumbore and James R. Randerson: Controls over carbon storage and  
714 turnover in high-latitude soils, *Global change biology*, 6, 196-210, 2000.

715 Schimel, D. S., House, J. I., Hibbard, K. A., Bousquet, P., Ciais, P., Peylin, P., Braswell, B. H., Apps, M.  
716 J., Baker, D., Bondeau, A., Canadell, J., Churkina, G., Cramer, W., Denning, A. S., Field, C. B.,  
717 Friedlingstein, P., Goodale, C., Heimann, M., Houghton, R. A., Melillo, J. M., III, B. M., Murdiyarso, D.,  
718 Noble, I., Pacala, S. W., Prentice, I. C., Raupach, M. R., Rayner, P. J., Scholes, R. J., Steffen, W. L., and  
719 Wirth, C.: Recent patterns and mechanisms of carbon exchange by terrestrial ecosystems, *Nature*, 414,  
720 2001.

721 Serreze, M. C., and Francis, J. A.: The Arctic on the fast track of change, *Weather*, 61, 65-69, 2006.

722 Shetler, G., Turetsky, M. R., Kane, E., and Kasischke, E.: Sphagnum mosses limit total carbon  
723 consumption during fire in Alaskan black spruce forests, *Canadian Journal of Forest Research*, 38, 2328-  
724 2336, 10.1139/x08-057, 2008.

725 Soja, A. J., Tchepakova, N. M., French, N. H. F., Flannigan, M. D., Shugart, H. H., Stocks, B. J.,  
726 Sukhinin, A. I., Parfenova, E. I., Chapin, F. S., and Stackhouse, P. W.: Climate-induced boreal forest  
727 change: Predictions versus current observations, *Global and Planetary Change*, 56, 274-296,  
728 10.1016/j.gloplacha.2006.07.028, 2007.

729 Stow, D. A., Hope, A., McGuire, D., Verbyla, D., Gamon, J., Huemmrich, F., Houston, S., Racine, C.,  
730 Sturm, M., Tape, K., Hinzman, L., Yoshikawa, K., Tweedie, C., Noyle, B., Silapaswan, C., Douglas, D.,  
731 Griffith, B., Jia, G., Epstein, H., Walker, D., Daeschner, S., Petersen, A., Zhou, L., and Myneni, R.:

732 Remote sensing of vegetation and land-cover change in Arctic Tundra Ecosystems, *Remote Sensing of*  
733 *Environment*, 89, 281-308, 10.1016/j.rse.2003.10.018, 2004.

734 T. G. Williams, L. B. F.: Measuring and modelling environmental influences on photosynthetic gas  
735 exchange in Sphagnum and Pleurozium, *Plant, Cell and Environment*, 21, 555–564, 1998.

736 Tang, J., and Zhuang, Q.: Equifinality in parameterization of process-based biogeochemistry models: A  
737 significant uncertainty source to the estimation of regional carbon dynamics, *Journal of Geophysical*  
738 *Research: Biogeosciences*, 113, 10.1029/2008jg000757, 2008.

739 Tape, K. E. N., Sturm, M., and Racine, C.: The evidence for shrub expansion in Northern Alaska and the  
740 Pan-Arctic, *Global change biology*, 12, 686-702, 10.1111/j.1365-2486.2006.01128.x, 2006.

741 Tarnocai, C., Canadell, J. G., Schuur, E. A. G., Kuhry, P., Mazhitova, G., and Zimov, S.: Soil organic  
742 carbon pools in the northern circumpolar permafrost region, *Global Biogeochemical Cycles*, 23, n/a-n/a,  
743 10.1029/2008gb003327, 2009.

744 Todd-Brown, K. E. O., Randerson, J. T., Post, W. M., Hoffman, F. M., Tarnocai, C., Schuur, E. A. G., and  
745 Allison, S. D.: Causes of variation in soil carbon simulations from CMIP5 Earth system models and  
746 comparison with observations, *Biogeosciences*, 10, 1717-1736, 10.5194/bg-10-1717-2013, 2013.

747 Treseder, K. K., Balser, T. C., Bradford, M. A., Brodie, E. L., Dubinsky, E. A., Eviner, V. T., Hofmockel,  
748 K. S., Lennon, J. T., Levine, U. Y., MacGregor, B. J., Pett-Ridge, J., and Waldrop, M. P.: Integrating  
749 microbial ecology into ecosystem models: challenges and priorities, *Biogeochemistry*, 109, 7-18,  
750 10.1007/s10533-011-9636-5, 2011.

751 Treseder, K. K., Marusenko, Y., Romero-Olivares, A. L., and Maltz, M. R.: Experimental warming alters  
752 potential function of the fungal community in boreal forest, *Global change biology*, 22, 3395-3404,  
753 10.1111/gcb.13238, 2016.

754 Turetsky, M. R., Mack, M. C., Hollingsworth, T. N., and Harden, J. W.: The role of mosses in ecosystem  
755 succession and function in Alaska's boreal forest This article is one of a selection of papers from The  
756 *Dynamics of Change in Alaska's Boreal Forests: Resilience and Vulnerability in Response to Climate*  
757 *Warming*, *Canadian Journal of Forest Research*, 40, 1237-1264, 10.1139/x10-072, 2010.

758 Turetsky, M. R., Bond-Lamberty, B., Euskirchen, E., Talbot, J., Frohling, S., McGuire, A. D., and Tuittila,  
759 E. S.: The resilience and functional role of moss in boreal and arctic ecosystems, *The New phytologist*,  
760 196, 49-67, 10.1111/j.1469-8137.2012.04254.x, 2012.

761 Wardle, M.-C. N. a. D. A.: Understory vegetation as a forest ecosystem driver: evidence from the northern  
762 Swedish boreal forest, *The Ecological Society of America*, 3, 421–428, 2005.

763 White, A., Cannell, M. G. R., and Friend, A. D.: The high-latitude terrestrial carbon sink: a model analysis  
764 *Global change biology*, 6, 227-245, 2000.

765 Wieder, W. R., Bonan, G. B., and Allison, S. D.: Global soil carbon projections are improved by  
766 modelling microbial processes, *Nature Climate Change*, 3, 909-912, 10.1038/nclimate1951, 2013.

767 Zha, J., and Zhuang, Q.: Microbial decomposition processes and vulnerable Arctic soil organic carbon in  
768 the 21st century, *Biogeosciences Discussions*, 1-34, 10.5194/bg-2018-241, 2018.

769 Zhuang, Q., Romanovsky, V. E., and McGuire, A. D.: Incorporation of a permafrost model into a large-  
770 scale ecosystem model: Evaluation of temporal and spatial scaling issues in simulating soil thermal  
771 dynamics, *Journal of Geophysical Research: Atmospheres*, 106, 33649-33670, 10.1029/2001jd900151,  
772 2001.

773 Zhuang, Q., McGuire, A. D., O'Neill, K. P., Harden, J. W., Romanovsky, V. E., and Yarie, J.: Modeling  
774 soil thermal and carbon dynamics of a fire chronosequence in interior Alaska, *Journal of Geophysical  
775 Research*, 108, 10.1029/2001jd001244, 2002.

776 Zhuang, Q., A. D. McGuire, J. M. Melillo, J. S. Clein, R. J. Dargaville, D. W. Kicklighter, R. B. Myneni,  
777 J. Dong, V. E. Romanovsky, J. Harden, J. E. Hobbie (2003) Carbon cycling in extratropical terrestrial  
778 ecosystems of the Northern Hemisphere during the 20th Century: A modeling analysis of the influences of  
779 soil thermal dynamics, *Tellus*, 55B, 751-776, 2003

780 Zhuang, Q., He, J., Lu, Y., Ji, L., Xiao, J., and Luo, T.: Carbon dynamics of terrestrial ecosystems on the  
781 Tibetan Plateau during the 20th century: an analysis with a process-based biogeochemical model, *Global  
782 Ecology and Biogeography*, 19, 649-662, 10.1111/j.1466-8238.2010.00559.x, 2010.

783 Zhuang, Q., Chen, M., Xu, K., Tang, J., Saikawa, E., Lu, Y., Melillo, J. M., Prinn, R. G., and McGuire, A.  
784 D.: Response of global soil consumption of atmospheric methane to changes in atmospheric climate and  
785 nitrogen deposition, *Global Biogeochemical Cycles*, 27, 650-663, 10.1002/gbc.20057, 2013.

786 Zhuang, Q., Zhu, X., He, Y., Prigent, C., Melillo, J. M., David McGuire, A., Prinn, R. G., and Kicklighter,  
787 D. W.: Influence of changes in wetland inundation extent on net fluxes of carbon dioxide and methane in  
788 northern high latitudes from 1993 to 2004, *Environmental Research Letters*, 10, 095009, 10.1088/1748-  
789 9326/10/9/095009, 2015.

790

791

792

793

794

795

796



797 **Author contributions.** Q.Z. designed the study. J.Z. conducted model development, simulation  
798 and analysis. J.Z. and Q. Z. wrote the paper.

799 **Competing financial interests.** The submission has no competing financial interests.

800 **Materials & Correspondence.** Correspondence and material requests should be addressed to  
801 qzhuang@purdue.edu.

802

803

804

805

806

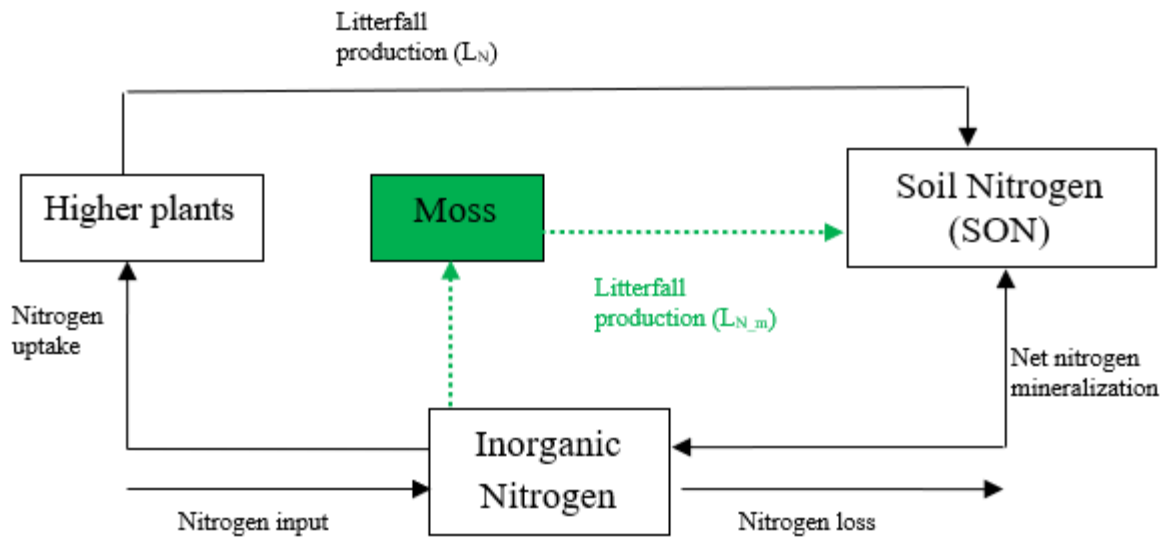
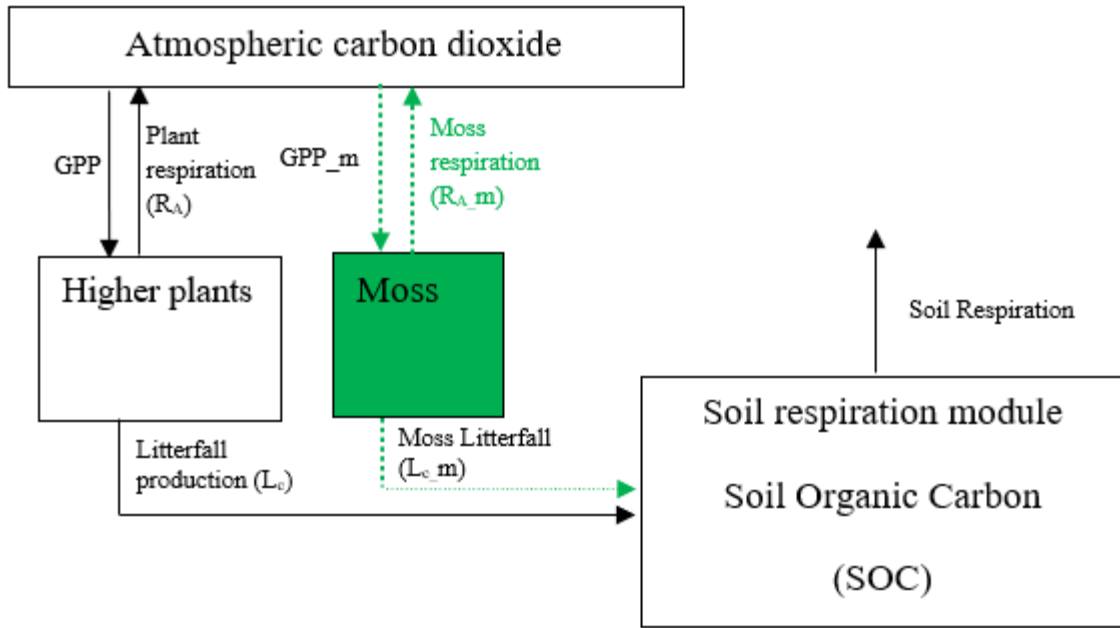
807

808

809

810

811

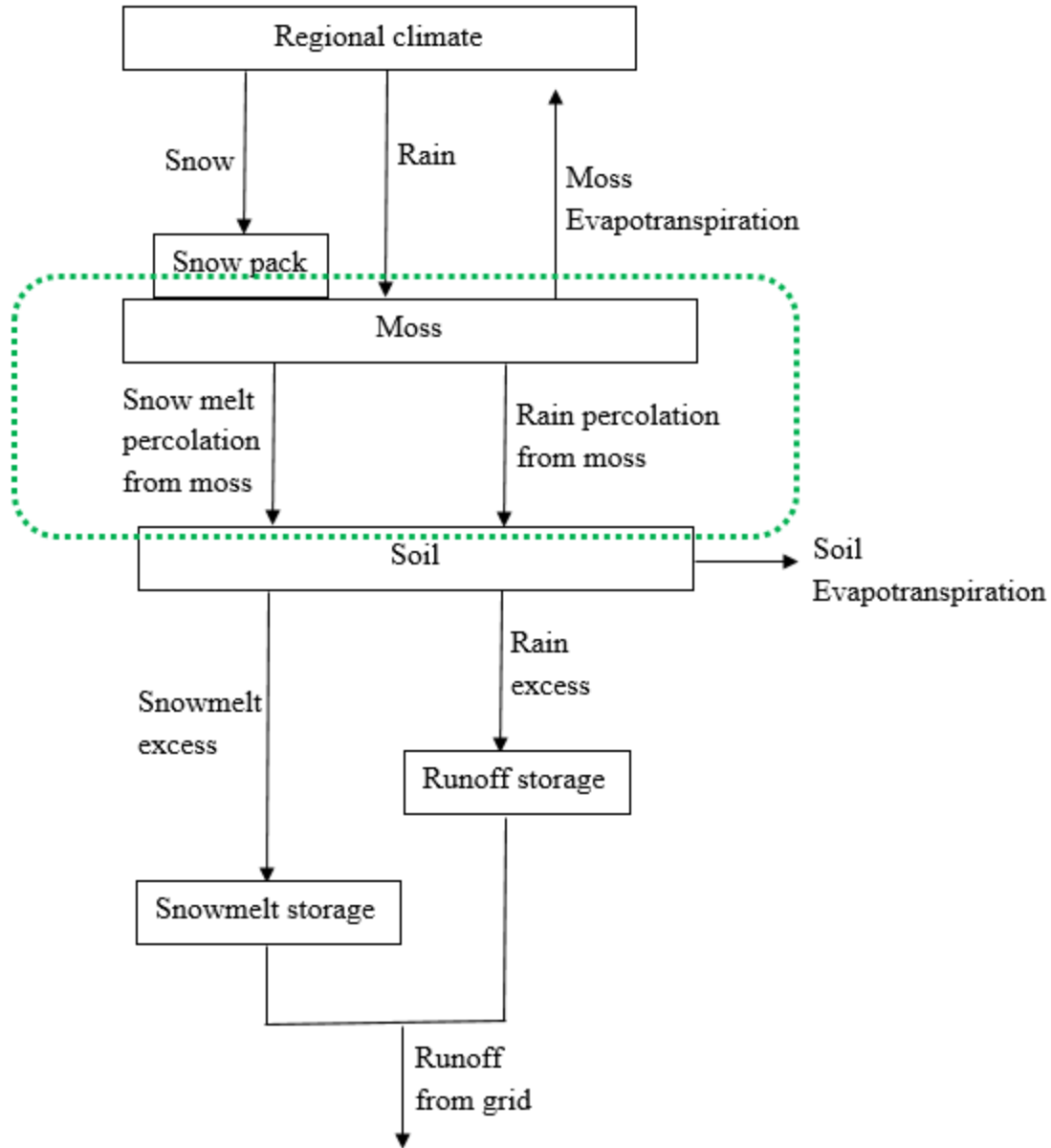


812

813 Figure 1. Schematic diagram of TEM\_Moss: Green dashed arrows are new carbon and nitrogen  
 814 fluxes, representing moss production, moss respiration and litterfall of moss. Black arrows were  
 815 in TEM 5.0 (Zhuang et al., 2013).

816

817



818

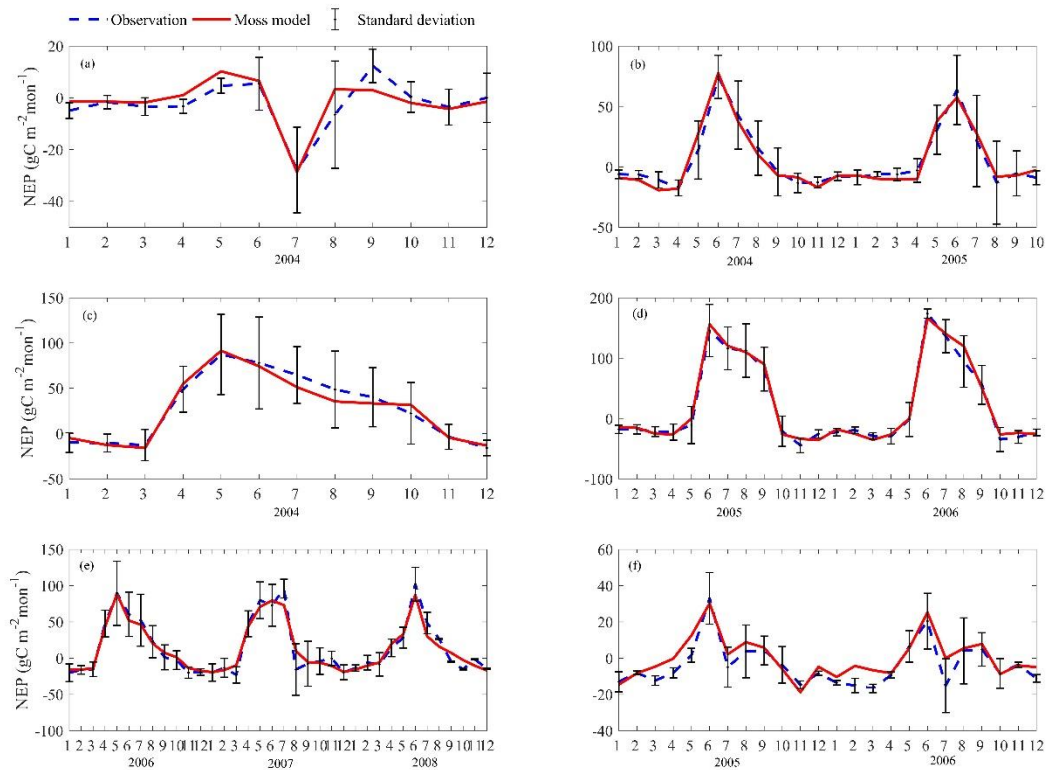
819 Figure 2. The revised Water Balance Model: Green dashed circle represents the hydrology  
 820 dynamics for moss (Vörösmarty et al., 1989).

821

822

823

824



825

826 Figure 3. Comparison between observed and simulated NEP ( $\text{gC m}^{-2}\text{mon}^{-1}$ ) at: (a) Iivotuk (alpine  
 827 tundra), (b) UCI-1964 burn site (boreal forest), (c) Howland Forest (main tower) (temperate  
 828 coniferous forest), (d) Univ. of Mich. Biological Station (Temperate deciduous forest), (e)  
 829 KUOM Turfgrass Field (Grassland), and (f) Atqasuk (Wet tundra). Note: scales are different.  
 830 Error bars represent standard errors among daily measure data in one month.

831

832

833

834

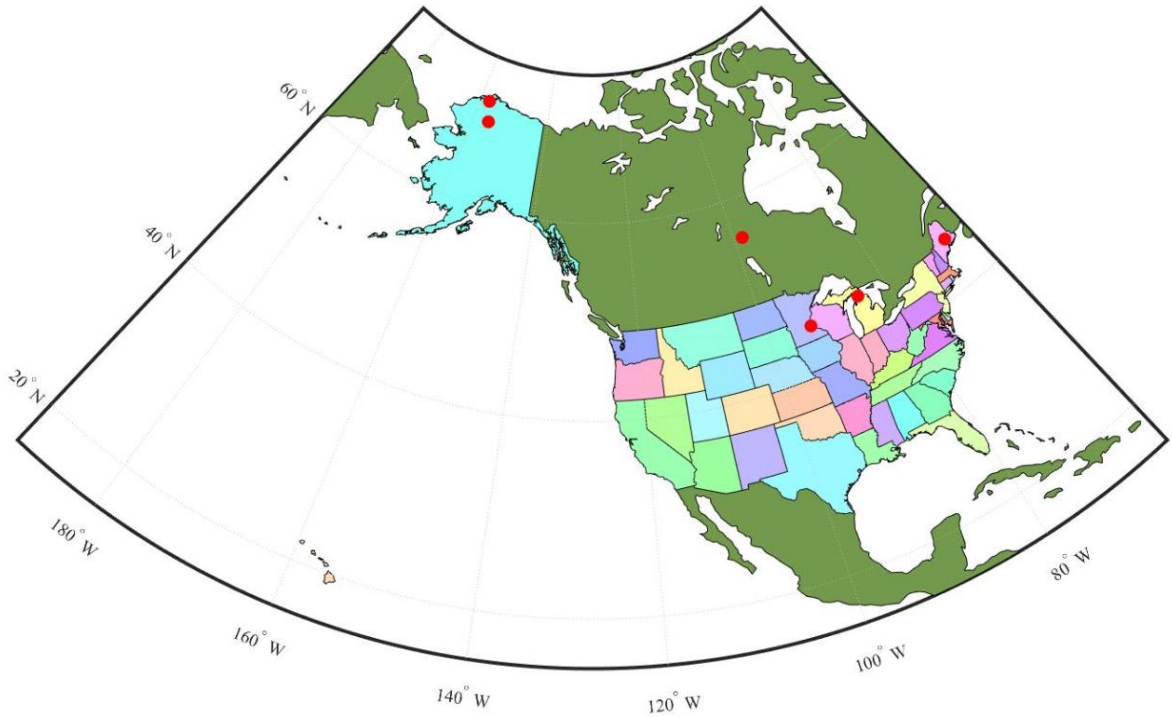
835

836

837

838

839



840

841 Figure 4. Map showing six sites used for TEM\_Moss calibration. The red points represent the six  
 842 sites, five are in the US and one is in the Canada: US-Ivo: Ivotuk (alpine tundra), CA-NS3: UCI-  
 843 1964 burn site (boreal forest), US-Ho1: Howland Forest (temperate coniferous forest), US-UMB:  
 844 Univ. of Mich. Biological Station (temperate deciduous forest), US-KUT: KUOM Turfgrass  
 845 Field (grassland), US-Atq: Atqasuk (wet tundra).

846

847

848

849

850

851

852

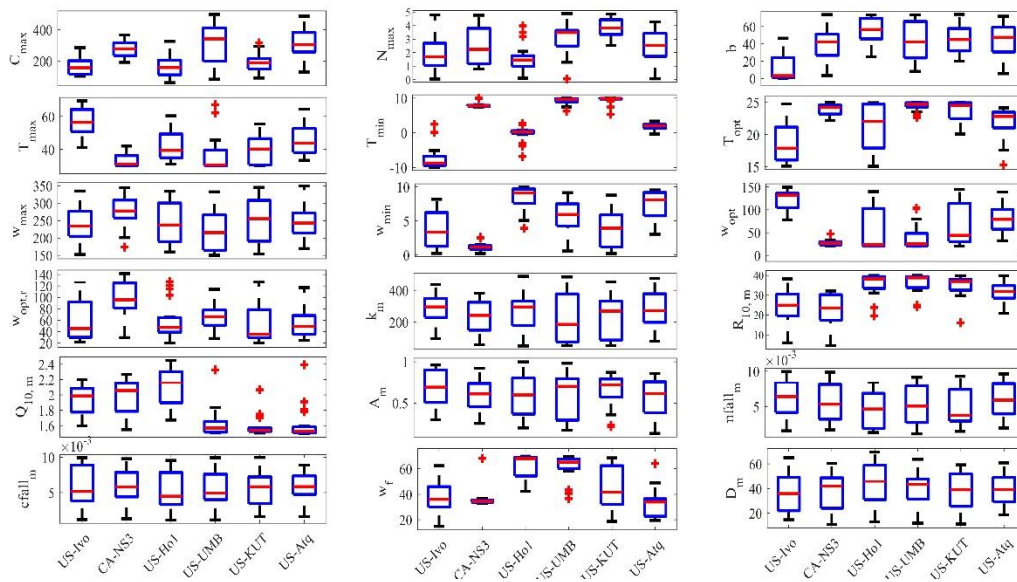
853

854

855

856

857



858

859 Figure 5. Boxplot of parameter posterior distribution that are obtained after ensemble inverse  
 860 modeling for TEM\_Moss at all six sites: US-Ivo: Ivotuk (alpine tundra), CA-NS3: UCI-1964  
 861 burn site (boreal forest), US-Hol: Howland Forest (temperate coniferous forest), US-UMB:  
 862 Univ. of Mich. Biological Station (temperate deciduous forest), US-KUT: KUOM Turfgrass  
 863 Field (grassland), US-Atq: Atqasuk (wet tundra). Boxes represent the range between the first  
 864 quartile and the third quartile of the parameter values, the red line within box represents the  
 865 second quartile or the mean of the values. The bottom and top whiskers represent minimum and  
 866 maximum parameter values, respectively.

867

868

869

870

871

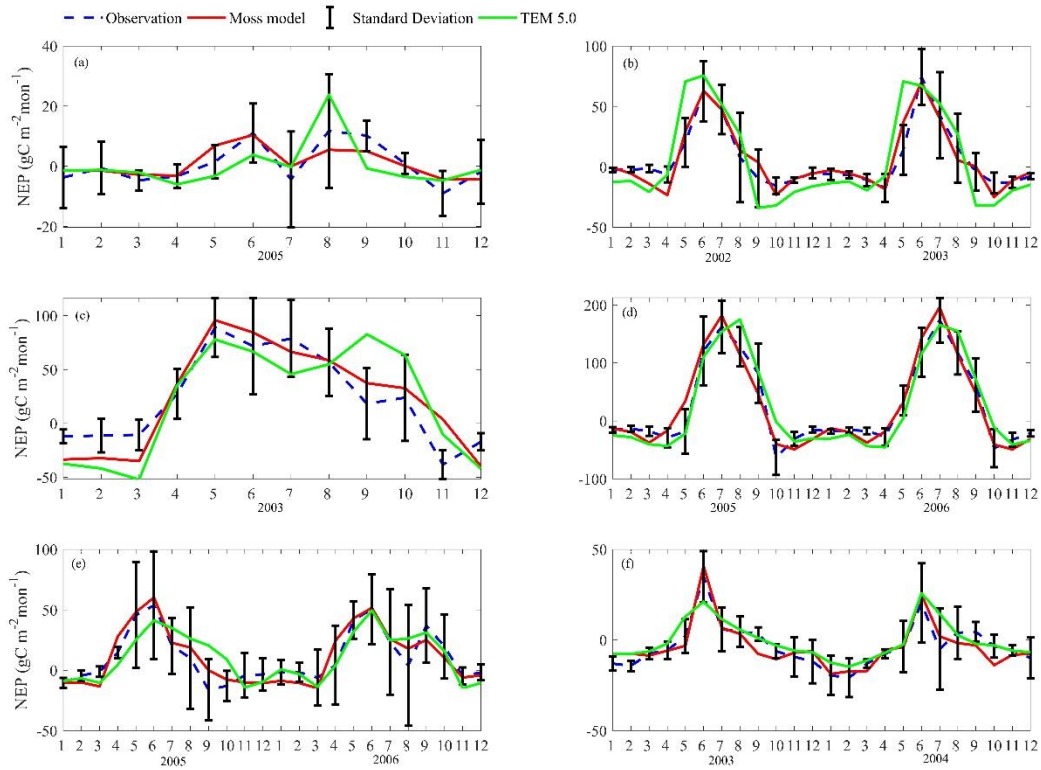
872

873

874

875

876



877

878 Figure 6. Comparison between observed and simulated NEP ( $\text{gC m}^{-2}\text{mon}^{-1}$ ) at: (a) Ivotuk (alpine  
 879 tundra), (b) UCI-1964 burn site (boreal forest), (c) Howland Forest (main tower) (temperate  
 880 coniferous forest), (d) Bartlett Experimental Forest (Temperate deciduous forest), (e) Brookings  
 881 (Grassland), and (f) Atqasuk (Wet tundra). Note: scales are different.

882

883

884

885

886

887

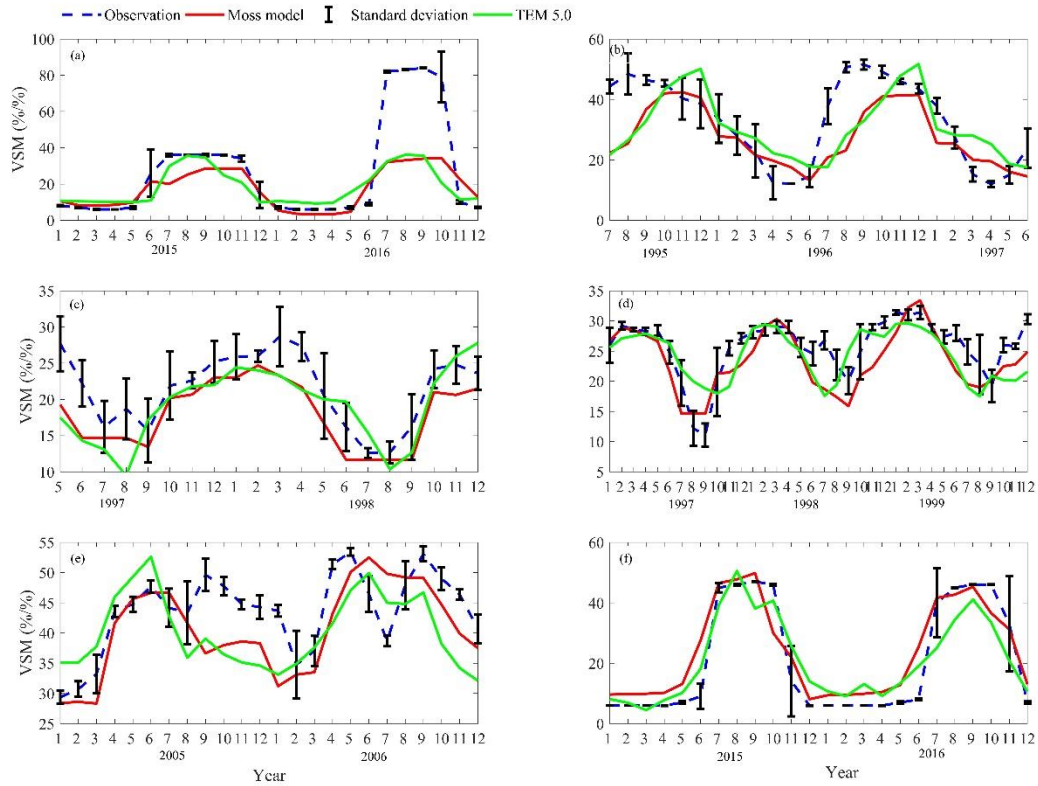
888

889

890

891

892



893

894 Figure 7. Comparison between observed and simulated volumetric soil moisture (VSM, %/%) at:  
 895 (a) US-Ivo (alpine tundra), (b) BOREAS NSA-OBS (boreal forest), (c) NL-Loo (temperate  
 896 coniferous forest), (d) DK-Sor (Temperate deciduous forest), (e) US-Bkg (Grassland), and (f)  
 897 US-Atq (Wet tundra). Note: scales are different.

898

899

900

901

902

903

904

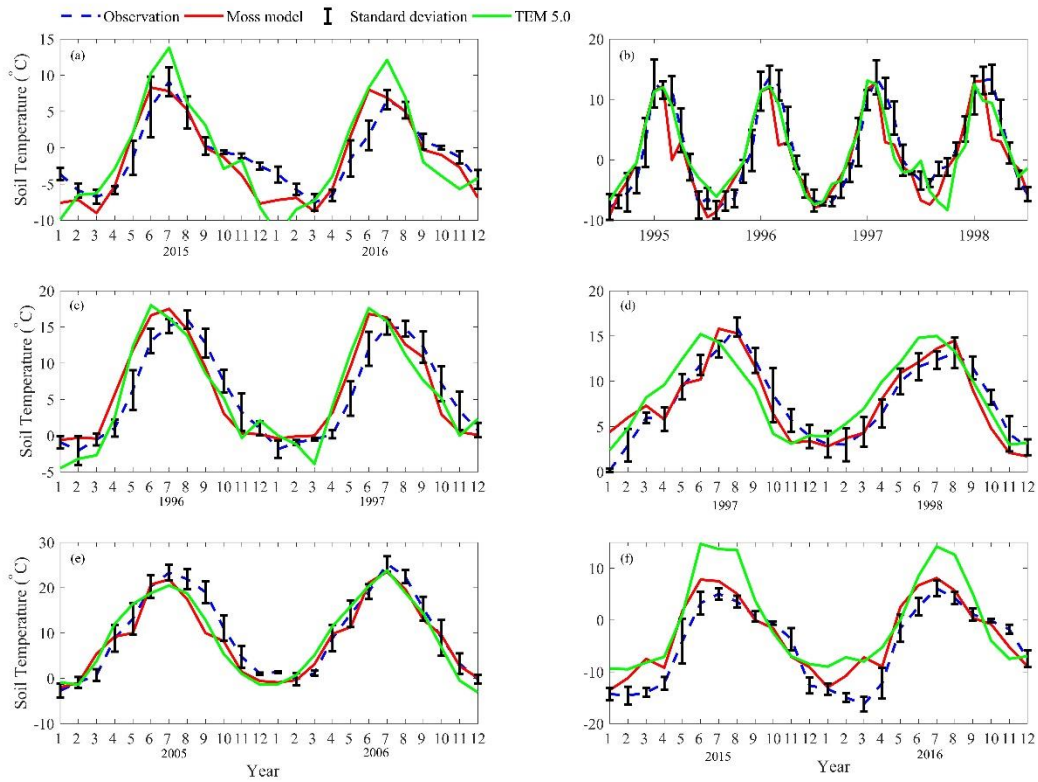
905

906

907

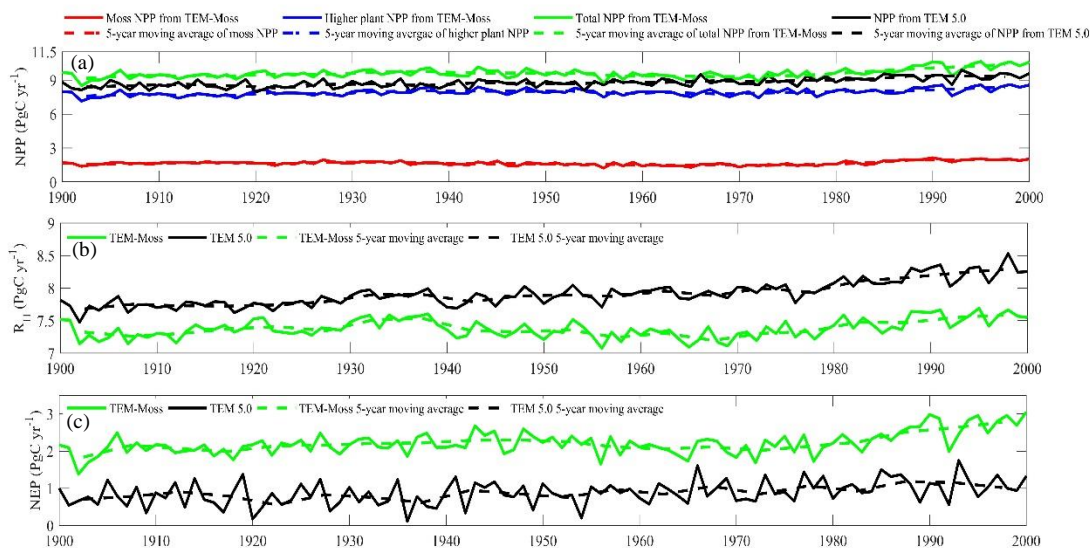
908





909  
 910 Figure 8. Comparison between observed and simulated soil temperature at 5cm depth (°C) at: (a)  
 911 US-Ivo (alpine tundra), (b) BOREAS NSA-OBS (boreal forest), (c) US-Ho1 (temperate  
 912 coniferous forest), (d) BE-Vie (Temperate deciduous forest), (e) US-Bkg (Grassland), and (f)  
 913 US-Atq (Wet tundra). Note: scales are different.

914  
 915  
 916  
 917  
 918  
 919  
 920  
 921  
 922  
 923  
 924  
 925



926

927 Figure 9. Simulated annual net primary production (NPP, a), heterotrophic respiration ( $R_H$ , b),  
 928 and net ecosystem production (NEP, c) during the 20<sup>th</sup> century by TEM\_Moss and TEM 5.0.

929

930

931

932

933

934

935

936

937

938

939

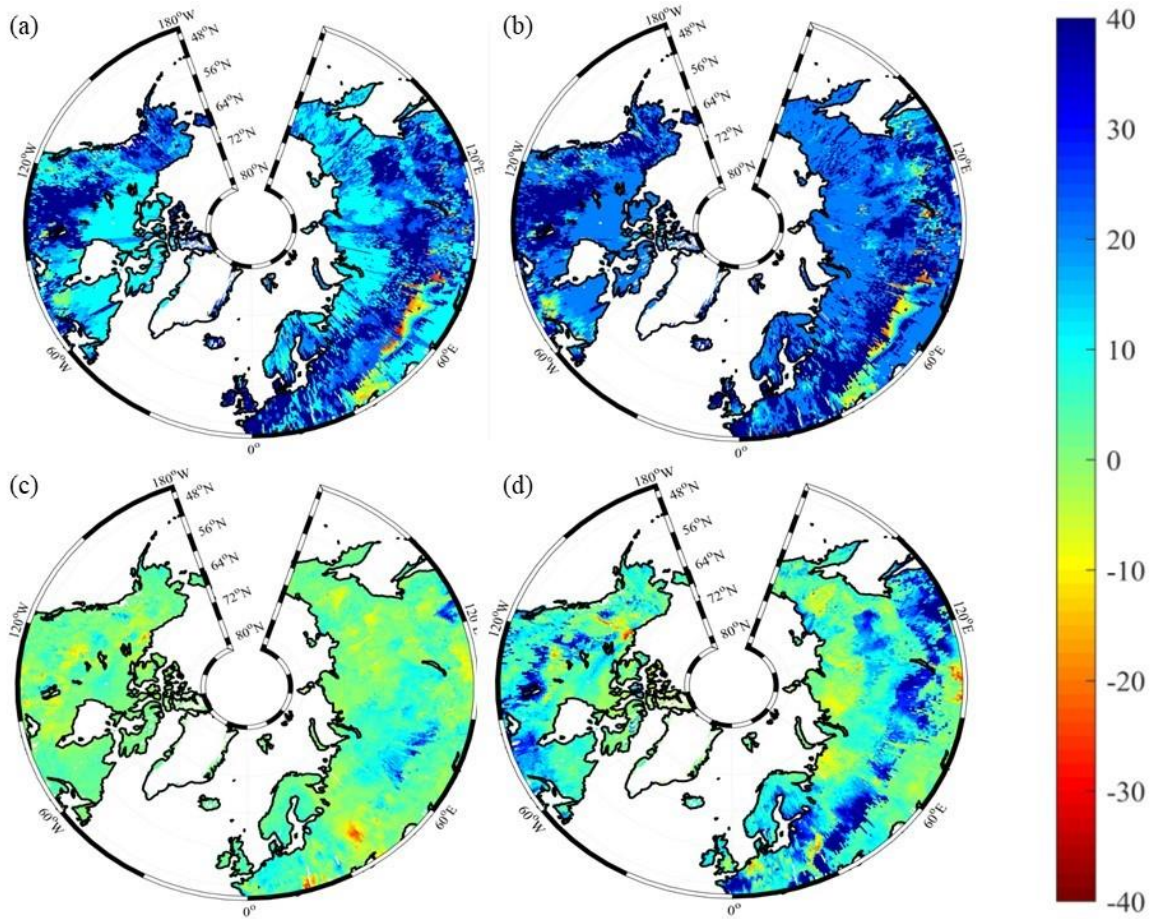
940

941

942

943

944



945

946 Figure 10. Spatial distribution of NEP simulated by TEM\_Moss for the periods (a) 1900–1950,  
 947 (b) 1951–2000, and by TEM 5.0 for the periods (c) 1900–1950, (d) 1951–2000. Positive values  
 948 of NEP represent sinks of CO<sub>2</sub> into terrestrial ecosystems, while negative values represent  
 949 sources of CO<sub>2</sub> to the atmosphere.

950

951

952

953

954

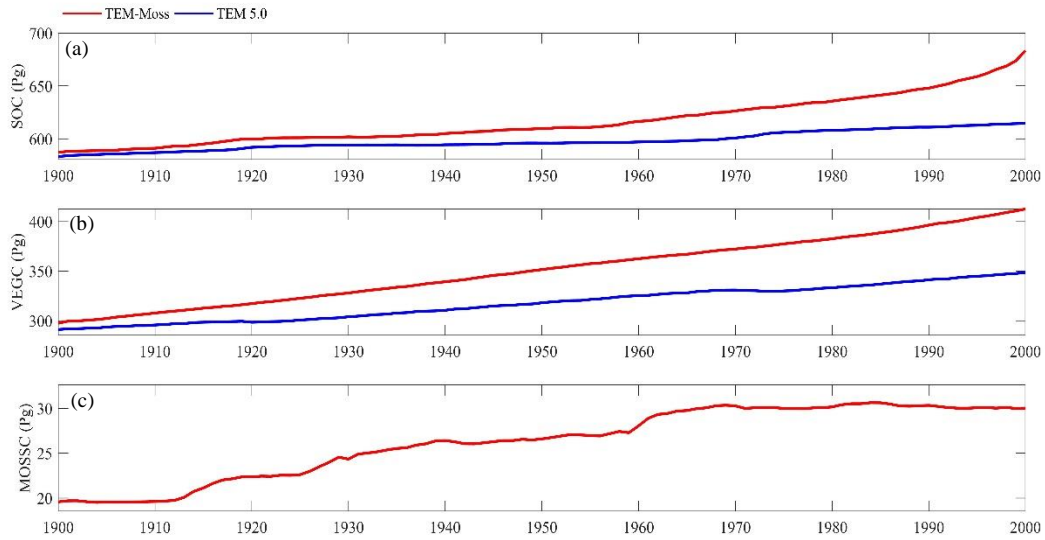
955

956

957

958

959



960

961 Figure 11. Simulated annual soil organic carbon (SOC, a), vegetation carbon (VEGC, b), and  
 962 moss carbon (MOSSC, c) during the 20<sup>th</sup> century by TEM\_Moss and TEM 5.0.

963

964

965

966

967

968

969

970

971

972

973

974

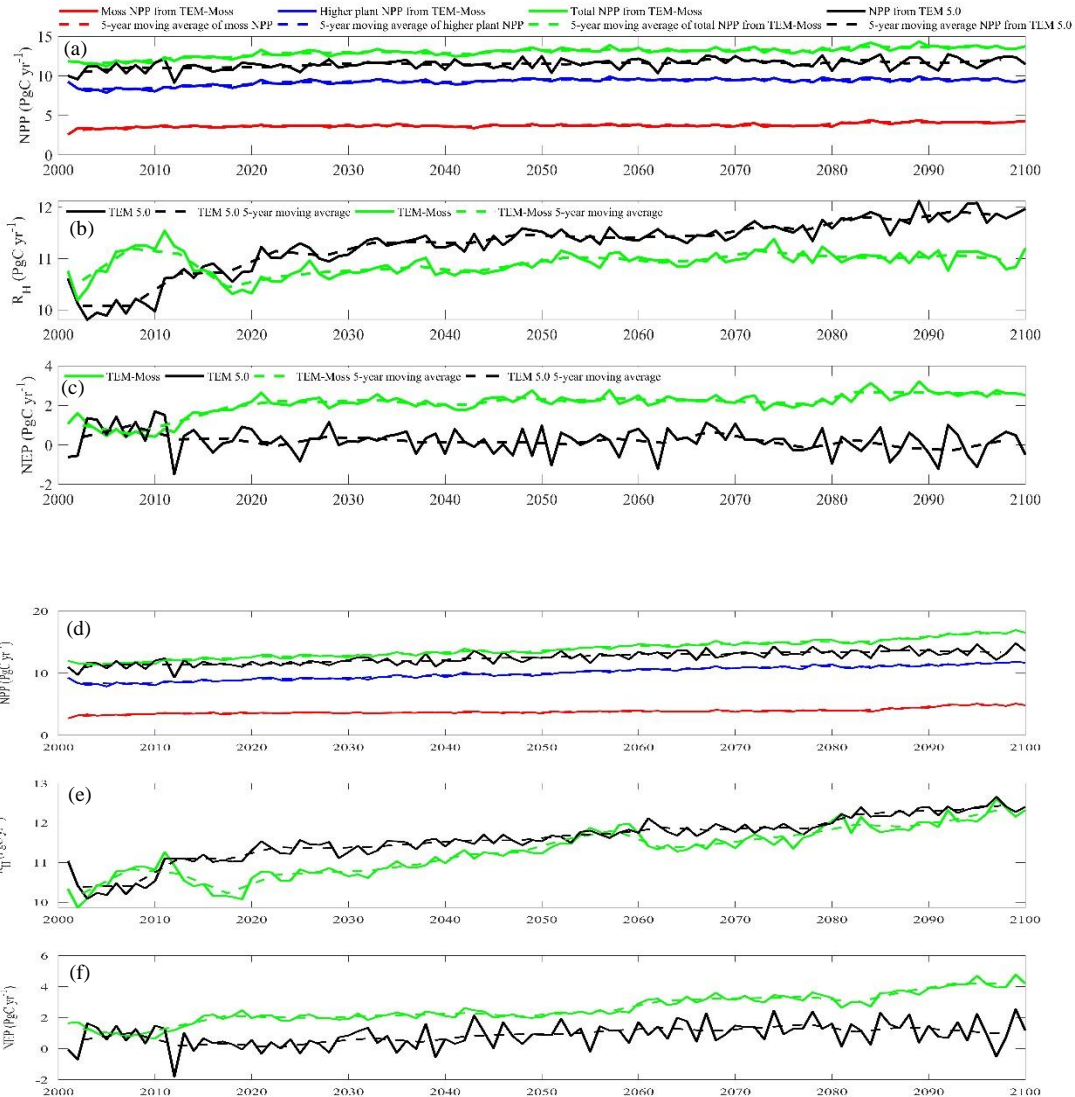
975

976

977

978

979



980

981  
 982 Figure 12. Predicted changes in carbon fluxes: annual net primary production (NPP, (a, d)),  
 983 heterotrophic respiration ( $R_H$ , (b, e)), and net ecosystem production (NEP, (c, f)) during the 21<sup>st</sup>  
 984 century under RCP 2.6 scenario (a, b, c, upper panel) and RCP 8.5 scenario (d, e, f, bottom  
 985 panel) by TEM\_Moss and TEM 5.0.

986

987

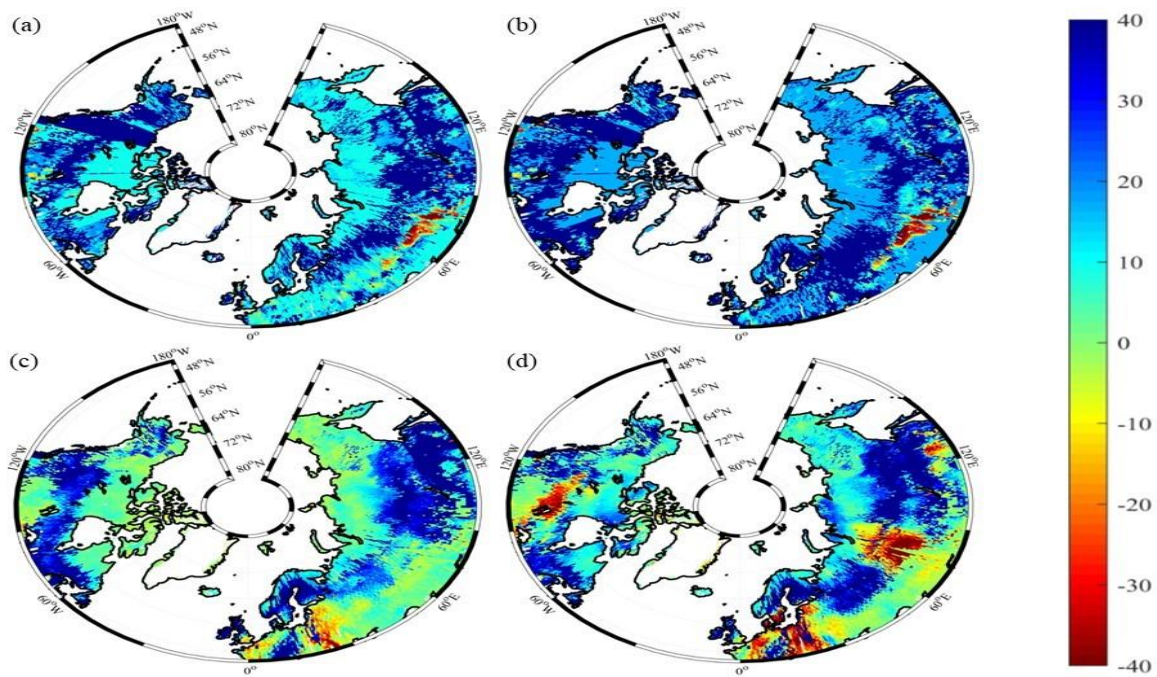
988

989

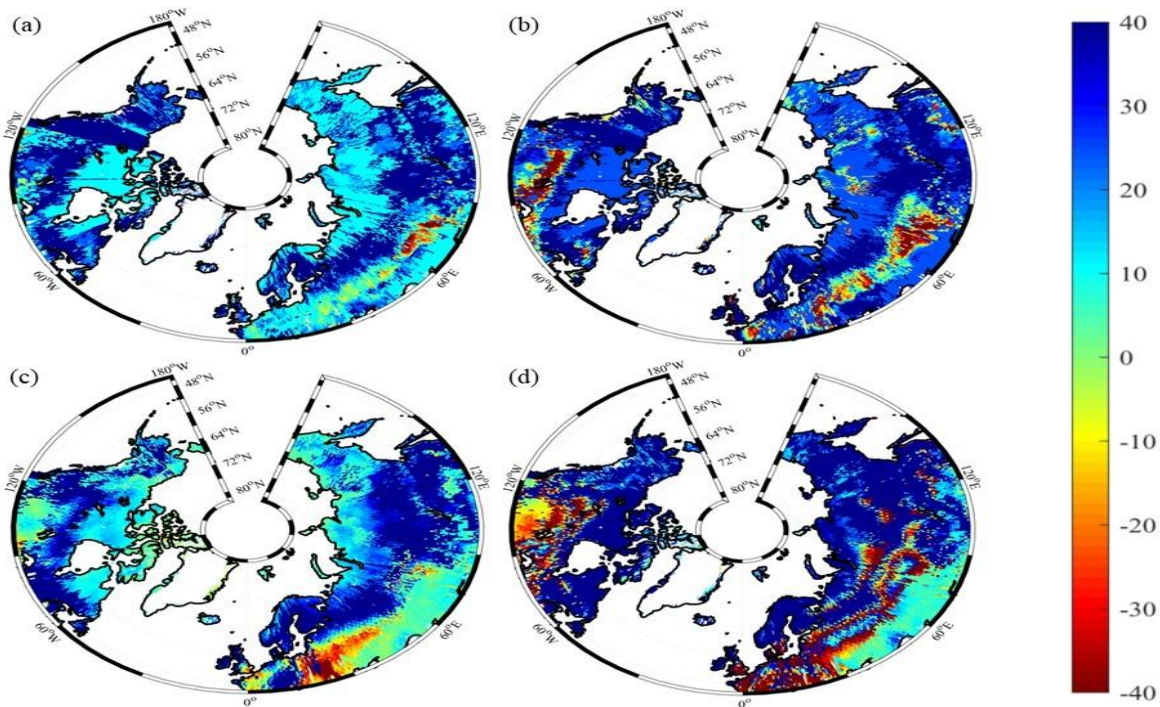
990

991

992



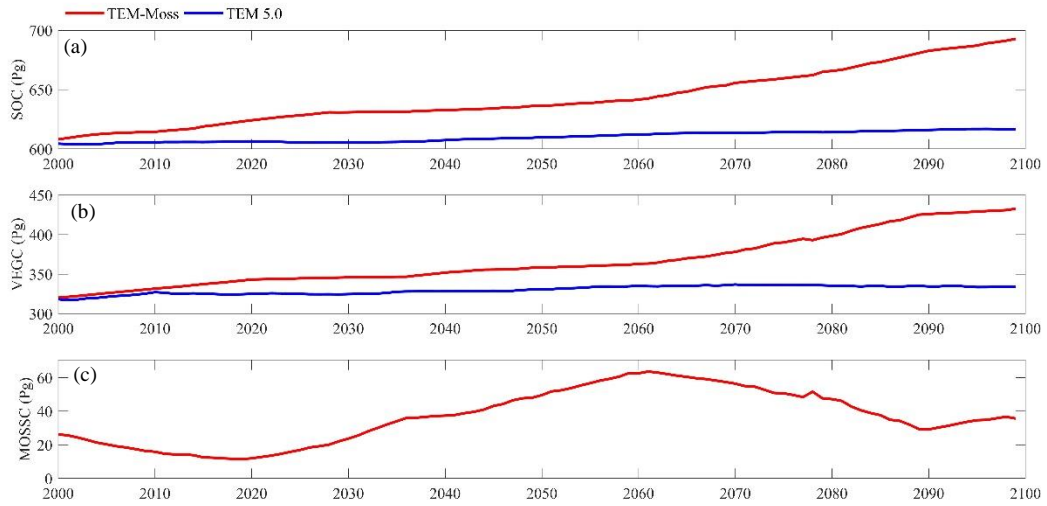
993



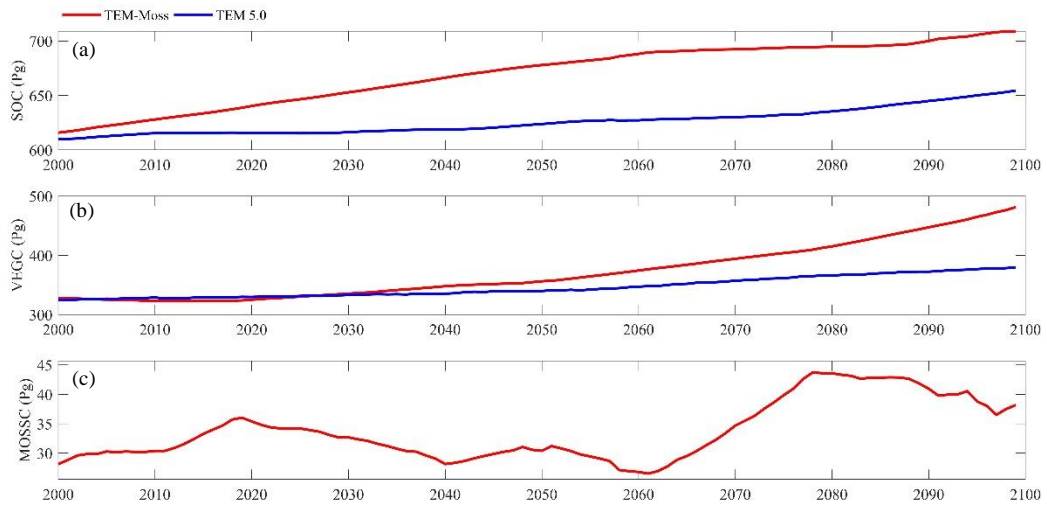
994

995 Figure 13. Spatial distribution of NEP simulated for the periods (a) 2000–2050, (b) 2051–2099  
996 by TEM\_Moss, and by TEM 5.0 (c, d) during the 21<sup>st</sup> century under RCP 2.6 scenario (upper  
997 panel) and RCP 8.5 scenario (bottom panel). Positive values of NEP represent sinks of CO<sub>2</sub> into  
998 terrestrial ecosystems, while negative values represent sources of CO<sub>2</sub> to the atmosphere.

999



1000



1001

1002 Figure 14. Simulated annual soil organic carbon (SOC, a), vegetation carbon (VEGC, b), and  
 1003 moss carbon (MOSSC, c) during the 21<sup>st</sup> century by TEM\_Moss and TEM 5.0 under RCP 2.6  
 1004 scenario (upper panel) and RCP 8.5 scenario (bottom panel).

1005

1006

1007

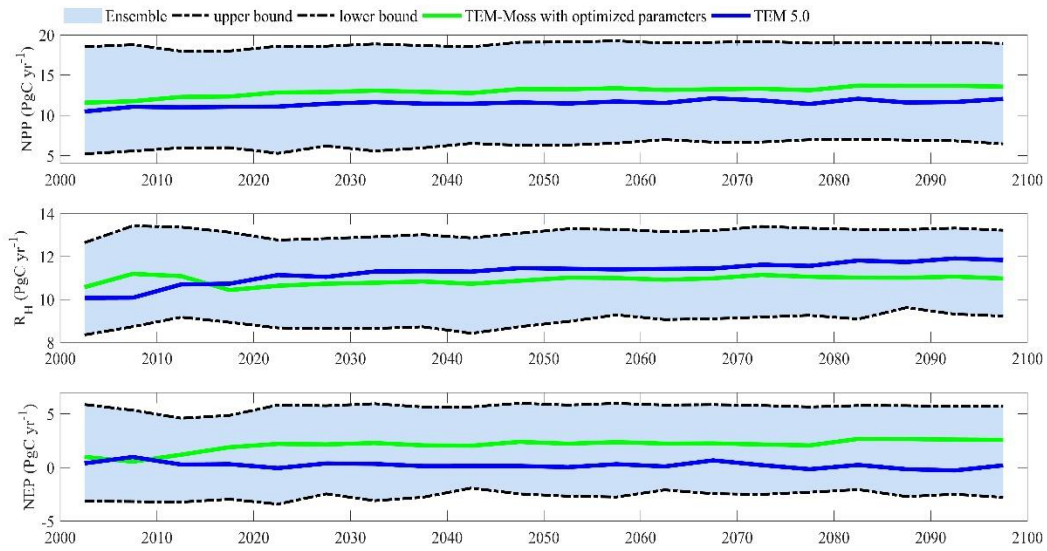
1008

1009

1010

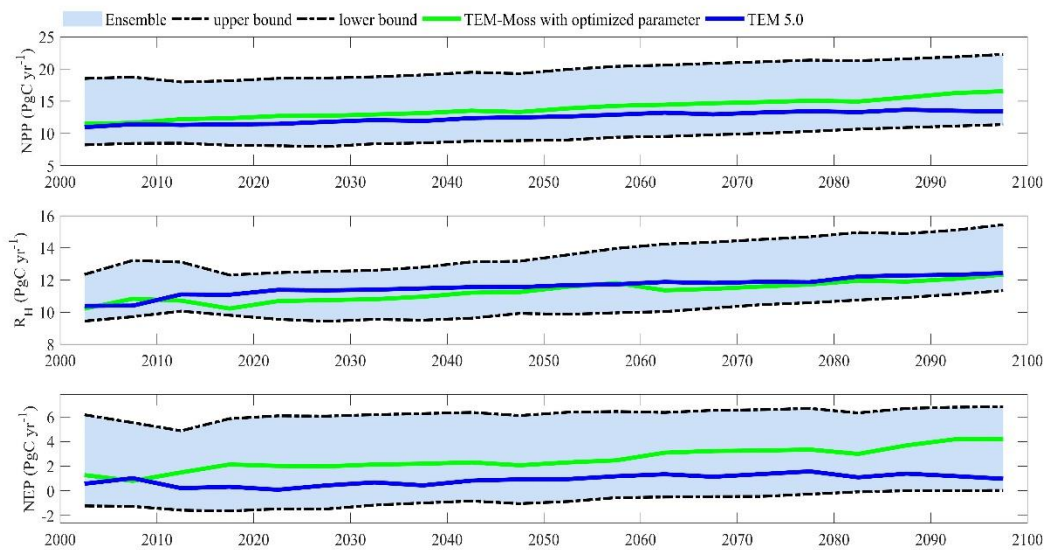
1011

1012 (a)



1013

1014 (b)



1015

1016 Figure 15. 5-year moving average plots for carbon fluxes under the (a) RCP 2.6 scenario and (b)  
1017 RCP 8.5 scenario. The blue area represents the upper and lower bounds of simulations.

1018

1019

1020



1021 **Table 1. Parameters associated with moss activities in TEM\_Moss**

| Parameter    | Units                    | descriptions  | Parameter range (value) | references                                  |
|--------------|--------------------------|---|-------------------------|---|
| $C_{max}$    | $gC\ m^{-2}$             | maximum rate of C assimilation                      | [50,500]                | Launiainen et al. (2015); Williams &        |
| $b$          | $\mu mol\ m^{-2}$        | Light half-saturation level                         | [5, 150]                | Launiainen et al. (2015); Raich et al.      |
| $T_{min}$    | $^{\circ}C$              | minimum temperature                                 | [-10, 10]               | Frolking et al. (1996); Raich et al. (1991) |
| $T_{max}$    | $^{\circ}C$              | maximum temperature                                 | [30, 80]                | Frolking et al. (1996); Raich et al. (1991) |
| $T_{opt}$    | $^{\circ}C$              | optimal temperature                                 | [15, 30]                | Frolking et al. (1996); Raich et al. (1991) |
| $w_{min}$    | mm                       | minimum water content for moss                      | [0.5, 15]               | Frolking et al. (1996); Launiainen et al.   |
| $w_{max}$    | mm                       | maximum water content for moss                      | [150, 380]              | Frolking et al. (1996); Launiainen et al.   |
| $w_{opt}$    | mm                       | optimal water content for moss                      | [10, 150]               | Frolking et al. (1996); Zhuang et al.       |
| $k_m$        | $\mu L/L$                | CO <sub>2</sub> concentration half-saturation level | [50, 500]               | Zhuang et al. (2002); Raich et al. (1991)   |
| $R_{10, m}$  | $gC\ m^{-2}$             | moss respiration rate at 10 °C                      | [0,40]                  | Frolking et al. (1996); Launiainen et al.   |
| $Q_{10, m}$  | -                        | moss respiration temperature sensitivity            | [1.5, 2.5]              | Frolking et al. (1996); Launiainen et al.   |
| $w_{opt, r}$ | mm                       | optimal water content for moss                      | [10, 150]               | Frolking et al., 1996; Zhuang et al.        |
| $c_{fall_m}$ | $g^{-1}g^{-1}\ mon^{-1}$ | constant proportion for carbon litterfall           | [0.001, 0.01]           | Zhuang et al. (2002); Raich et al. (1991)   |
| $N_{max}$    | $gN\ m^{-2}$             | maximum rate of N uptake by mosses                  | [0.1,5]                 | Zhuang et al. (2002); Raich et al. (1991)   |
| $k_n$        | $g\ m^{-2}$              | Half-saturation constant for N uptake by            | 1.0                     | Zhuang et al. (2002); Raich et al. (1991)   |
| $A_m$        | -                        | relative allocation of effort to C vs. N            | [0,1]                   | Raich et al. (1991)                         |
| $w_f$        | mm                       | moss field capacity                                 | [10, 80]                | Frolking et al. (1996); Raich et al. (1991) |
| $n_{fall_m}$ | $g^{-1}g^{-1}\ mon^{-1}$ | constant proportion for nitrogen litterfall         | [0.001, 0.01]           | Zhuang et al. (2002); Raich et al. (1991)   |
| $D_m$        | mm                       | Moss thickness                                      | [0, 100]                | Zhuang et al. (2002)                        |

**Table 2. Site description and measured NEP data used to calibrate TEM\_Moss**

| Site Name                                  | Location<br>(Longitude<br>(degrees)<br>/Latitude<br>(degrees)) | Elevation<br>(m) | Vegetation<br>type                | Description  | Data<br>range       | Citations                 |
|--|--|------------------|-----------------------------------|--|---------------------|---------------------------|
| Univ. of<br>Mich.<br>Biological<br>Station | 84.71W<br>45.56 N  | 234              | Temperate<br>deciduous<br>forest  | Located within a protected forest owned<br>by the University of Michigan. Mean<br>annual temperature is 5.83° C with mean<br>annual precipitation of 803mm | 01/2005-<br>12/2006 | Gough et al.<br>(2013)    |
| Howland<br>Forest (main<br>tower)          | 68.74W<br>45.20N   | 60               | Temperate<br>coniferous<br>forest | Closed coniferous forest, minimal<br>disturbance.  | 01/2004-<br>12/2004 | Davidson et al.<br>(2006) |
| UCI-1964<br>burn site                      | 98.38W<br>55.91N   | 260              | Boreal<br>forest                  | Located in a continental boreal forest,<br>dominated by black spruce trees, within<br>the BOREAS northern study area in<br>central Manitoba, Canada.       | 01/2004-<br>10/2005 | Goulden et al.<br>(2006)  |
| KUOM<br>Turfgrass<br>Field                 | 93.19W<br>45.0N  | 301              | Grassland                         | A low-maintenance lawn consisting of<br>cool-season turfgrasses.   | 01/2006-<br>12/2008 | Hiller et al. (2010)      |
| Atqasuk                                    | 157.41W<br>70.47N  | 15               | Wet tundra                        | 100 km south of Barrow, Alaska. Variety<br>of moist-wet coastal sedge tundra, and<br>moist-tussock tundra surfaces in the more<br>well-drained upland.     | 01/2005-<br>12/2006 | Oechel et al.<br>(2014);  |
| Ivotuk                                     | 155.75W<br>68.49N  | 568              | Alpine<br>tundra                  | 300 km south of Barrow and is located at<br>the foothill of the Brooks Range and is<br>classified as tussock sedge, dwarf-shrub,<br>moss tundra.           | 01/2004-<br>12/2004 | McEwing et al.<br>(2015)  |

**Table 3. Site description and measured NEP data used to validate TEM\_Moss**

| Site Name                          | Location<br>(Longitude<br>(degrees)<br>/Latitude<br>(degrees)) | Elevation<br>(m) | Vegetation<br>type                | Description  | Data<br>range       | Citations  |
|------------------------------------|--|------------------|-----------------------------------|--|---------------------|--|
| Bartlett<br>Experimental<br>Forest | 71.29W/<br>44.06N  | 272              | Temperate<br>deciduous<br>forest  | Located within the White Mountains National Forest in north-central New Hampshire, USA, with mean annual temperature of 5.61 °C and mean annual precipitation of 1246mm.   | 01/2005-<br>12/2006 | Jenkins et al.<br>(2007);<br>Richardson et al.<br>(2007) |
| Howland<br>Forest (main<br>tower)  | 68.74W/<br>45.20N  | 60               | Temperate<br>coniferous<br>forest | Closed coniferous forest, minimal disturbance.   | 01/2003-<br>12/2003 | Davidson et al.<br>(2006)                                |
| UCI-1964 burn<br>site              | 98.38W/<br>55.91N  | 260              | Boreal<br>forest                  | Located in a continental boreal forest, dominated by black spruce trees, within the BOREAS northern study area in central Manitoba, Canada.  | 01/2002-<br>12/2003 | Goulden et al.<br>(2006)                                 |
| Brookings                          | 96.84W/<br>44.35N  | 510              | Grassland                         | Located in a private pasture, belonging to the Northern Great Plains Rangelands, the grassland is representative of many in the north central United States, with seasonal winter conditions and a wet growing season. | 01/2005-<br>12/2006 | Gilmanov et al.<br>(2005)                                |
| Atqasuk                            | 157.41W<br>/<br>70.47N   | 15               | Wet tundra                        | 100 km south of Barrow, Alaska. Variety of moist-wet coastal sedge tundra, and moist-tussock tundra surfaces in the more well-drained upland.  | 01/2003-<br>12/2004 | Oechel et al.<br>(2014);                                 |
| Ivotuk                             | 155.75W<br>/<br>68.49N   | 568              | Alpine<br>tundra                  | 300 km south of Barrow and is located at the foothill of the Brooks Range and is classified as tussock sedge, dwarf-shrub, moss tundra.  | 01/2005-<br>12/2005 | McEwing et al.<br>(2015)                                 |

**Table 4. Site description and measured volumetric soil moisture data used to validate TEM\_Moss**

| Site              | Location<br>(Longitude (degrees)<br>/Latitude (degrees)) | Elevation<br>(m) | Vegetation type                | Data range          | Citations               |
|-------------------|--|------------------|--------------------------------|---------------------|-------------------------|
| US-Ivo            | 155.75W/<br>68.49N                                       | 579              | Alpine tundra                  | 01/2015-<br>12/2016 | Oechel & Kalhori (2018) |
| BOREAS<br>NSA-OBS | 98.48W/<br>55.88N  | 259              | Boreal forest                  | 07/1995-<br>06/1997 | Stangel & Kelly (1999)  |
| NL-Loo            | 5.74E/<br>52.17N   | 25               | Temperate coniferous<br>forest | 05/1997-<br>12/1998 | Falge et al. (2005)     |
| DK-Sor            | 11.64E/<br>55.49N  | 40               | Temperate deciduous<br>forest  | 01/1997-<br>12/1999 | Falge et al. (2005)     |
| US-Bkg            | 96.84W/<br>44.35N  | 510              | Grasslands                     | 01/2005-<br>12/2006 | Gilmanov et al. (2005)  |
| US-Atq            | 157.41W/<br>70.47N                                       | 25               | Wet tundra                     | 01/2015-<br>12/2016 | Oechel & Kalhori (2018) |

**Table 5. Site description and measured soil temperature at 5cm depth data used to validate TEM\_Moss**

| Site              | Location<br>(Longitude (degrees)<br>/Latitude (degrees)) | Elevation<br>(m) | Vegetation type                | Data range          | Citations               |
|-------------------|--|------------------|--------------------------------|---------------------|-------------------------|
| US-Ivo            | 155.75W/<br>68.49N                                       | 579              | Alpine tundra                  | 01/2015-<br>12/2016 | Oechel & Kalhori (2018) |
| BOREAS<br>NSA-OBS | 98.48W/<br>55.88N  | 259              | Boreal forest                  | 01/1995-<br>12/1998 | Stangel & Kelly (1999)  |
| US-Ho1            | 68.74W/<br>45.2N   | 60               | Temperate coniferous<br>forest | 01/1996-<br>12/1997 | Falge et al. (2005)     |
| BE-Vie            | 6.0E/<br>50.3N   | 493              | Temperate deciduous<br>forest  | 01/1997-<br>12/1998 | Falge et al. (2005)     |
| US-Bkg            | 96.84W/<br>44.35N  | 510              | Grasslands                     | 01/2005-<br>12/2006 | Gilmanov et al. (2005)  |
| US-Atq            | 157.41W/<br>70.47N                                       | 25               | Wet tundra                     | 01/2015-<br>12/2016 | Oechel & Kalhori (2018) |

**Table 6. Model validation statistics for TEM\_Moss and TEM 5.0 at six sites with NEP data**

| Site Name                    | Vegetation type             | Models   | Intercept | Slope | R-square | Adjusted R-square | RMSE  | p-value |
|------------------------------|-----------------------------|----------|-----------|-------|----------|-------------------|-------|---------|
| Ivotuk                       | Alpine tundra               | TEM_Moss | 0.46      | 0.61  | 0.72     | 0.70              | 3.57  | <0.001  |
|                              |                             | TEM 5.0  | -0.22     | 0.75  | 0.43     | 0.41              | 5.88  | 0.02    |
| UCI-1964 burn site           | Boreal forest               | TEM_Moss | -0.13     | 1.01  | 0.91     | 0.90              | 8.33  | <0.001  |
|                              |                             | TEM 5.0  | -2.45     | 1.29  | 0.75     | 0.74              | 20.1  | <0.001  |
| Howland Forest (main tower)  | Temperate coniferous forest | TEM_Moss | -1.28     | 1.05  | 0.83     | 0.81              | 19.69 | <0.001  |
|                              |                             | TEM 5.0  | -2.22     | 0.97  | 0.62     | 0.61              | 31.23 | 0.002   |
| Bartlett Experimental Forest | Temperate deciduous forest  | TEM_Moss | -0.49     | 1.03  | 0.94     | 0.94              | 19.06 | <0.001  |
|                              |                             | TEM 5.0  | -2.49     | 1.04  | 0.91     | 0.89              | 23    | <0.001  |
| Brookings                    | Grassland                   | TEM_Moss | 0.36      | 1.02  | 0.85     | 0.84              | 8.95  | <0.001  |
|                              |                             | TEM 5.0  | 2.58      | 0.75  | 0.62     | 0.6               | 13.07 | <0.001  |
| Atqasuk                      | Wet tundra                  | TEM_Moss | -0.36     | 0.97  | 0.84     | 0.83              | 5.13  | <0.001  |
|                              |                             | TEM 5.0  | 1.99      | 0.75  | 0.75     | 0.74              | 6.56  | <0.001  |

**Table 7. Model validation statistics for TEM\_Moss and TEM 5.0 at six sites with volumetric soil moisture data**

| Site ID           | Vegetation type                | Models   | Intercept | Slope | R-square | Adjusted R-square | RMSE  | p-value |
|-------------------|--------------------------------|----------|-----------|-------|----------|-------------------|-------|---------|
| US-Ivo            | Alpine tundra                  | TEM_Moss | 8.56      | 0.34  | 0.74     | 0.72              | 20.8  | <0.001  |
|                   |                                | TEM 5.0  | 10.67     | 0.29  | 0.64     | 0.62              | 21.76 | <0.001  |
| BOREAS<br>NSA-OBS | Boreal forest                  | TEM_Moss | 10.71     | 0.51  | 0.52     | 0.51              | 11.1  | <0.001  |
|                   |                                | TEM 5.0  | 16.47     | 0.43  | 0.32     | 0.31              | 11.96 | <0.001  |
| NL-Loo            | Temperate<br>coniferous forest | TEM_Moss | 0.47      | 0.82  | 0.83     | 0.81              | 4.0   | <0.001  |
|                   |                                | TEM 5.0  | 3.75      | 0.72  | 0.49     | 0.48              | 4.5   | <0.001  |
| DK-Sor            | Temperate<br>deciduous forest  | TEM_Moss | 1.39      | 0.86  | 0.67     | 0.65              | 3.65  | <0.001  |
|                   |                                | TEM 5.0  | 10.41     | 0.54  | 0.4      | 0.39              | 4.06  | <0.001  |
| US-Bkg            | Grassland                      | TEM_Moss | 5.64      | 0.8   | 0.51     | 0.49              | 6.05  | <0.001  |
|                   |                                | TEM 5.0  | 22.24     | 0.41  | 0.21     | 0.2               | 7.34  | 0.027   |
| US-Atq            | Wet tundra                     | TEM_Moss | 7.76      | 0.77  | 0.87     | 0.85              | 7.38  | <0.001  |
|                   |                                | TEM 5.0  | 6.74      | 0.68  | 0.85     | 0.84              | 7.63  | <0.001  |

**Table 8. Model validation statistics for TEM\_Moss and TEM 5.0 at six sites with soil temperature at 5cm depth data**

| Site ID           | Vegetation type                | Models   | Intercept | Slope | R-square | Adjusted R-square | RMSE | p-value |
|-------------------|--------------------------------|----------|-----------|-------|----------|-------------------|------|---------|
| US-Ivo            | Alpine tundra                  | TEM_Moss | -0.34     | 1.16  | 0.83     | 0.82              | 2.54 | <0.001  |
|                   |                                | TEM 5.0  | 0.54      | 1.36  | 0.75     | 0.73              | 3.94 | <0.001  |
| BOREAS<br>NSA-OBS | Boreal forest                  | TEM_Moss | -0.05     | 0.91  | 0.9      | 0.88              | 2.24 | <0.001  |
|                   |                                | TEM 5.0  | 0.27      | 0.81  | 0.84     | 0.82              | 2.9  | <0.001  |
| US-Ho1            | Temperate<br>coniferous forest | TEM_Moss | 0.7       | 0.95  | 0.81     | 0.79              | 2.93 | <0.001  |
|                   |                                | TEM 5.0  | -0.06     | 0.99  | 0.77     | 0.76              | 3.41 | <0.001  |
| BE-Vie            | Temperate<br>deciduous forest  | TEM_Moss | 0.57      | 0.92  | 0.83     | 0.81              | 1.82 | <0.001  |
|                   |                                | TEM 5.0  | 1.88      | 0.85  | 0.69     | 0.68              | 2.56 | <0.001  |
| US-Bkg            | Grassland                      | TEM_Moss | 0.17      | 0.87  | 0.91     | 0.89              | 2.87 | <0.001  |
|                   |                                | TEM 5.0  | -0.01     | 0.91  | 0.89     | 0.87              | 3.04 | <0.001  |
| US-Atq            | Wet tundra                     | TEM_Moss | 1.36      | 0.86  | 0.84     | 0.82              | 3.63 | <0.001  |
|                   |                                | TEM 5.0  | 4.33      | 0.99  | 0.75     | 0.74              | 6.17 | <0.001  |



**Table 9. Average annual NPP,  $R_H$  and NEP (as Pg C per year) during the 20<sup>th</sup> century estimated by two models.**

| Average annual carbon fluxes (PgC yr <sup>-1</sup> ) |                        | TEM_Moss | TEM 5.0 | Difference | Moss NPP/<br>Vascular plants<br>NPP |
|--|------------------------|----------|---------|------------|-------------------------------------|
| NPP  | Moss NPP               | 1.69     | -       | -          | 21.3%                               |
|  | Vascular plants<br>NPP | 7.93     | 8.8     | -          |                                     |
|  | Total NPP              | 9.6      | 8.8     | 0.8        |                                     |
| $R_H$  |                        | 7.38     | 7.91    | -0.53      |                                     |
| NEP  |                        | 2.22     | 0.89    | 1.33       |                                     |

**Table 10. Increasing of SOC, vegetation carbon (VGC), and moss carbon (MOSSC) from 1900 to 2000, and total carbon storage during the 20<sup>th</sup> century predicted by two models.**

| Models   | Carbon pools | Carbon pool amounts in 1900/2000 (units: Pg) | Changes in carbon pools during the 20 <sup>th</sup> century (units: Pg) |
|----------|--------------|--|---|
| TEM_Moss | SOC          | 587.1/683.4                                  | 96.3  |
|          | VEGC         | 297.5/412.7                                  | 115.2   |
|          | MOSSC        | 19.6/30                                      | 10.4  |
|          | Total        | 904.2/1126.1                                 | 221.9   |
| TEM 5.0  | SOC          | 583.2/614.9                                  | 31.7  |
|          | VEGC         | 291.1/348.6                                  | 57.5  |
|          | Total        | 874.3/963.5                                  | 89.2  |

**Table 11. Average annual NPP,  $R_H$  and NEP (as Pg C per year) during the 21<sup>st</sup> century estimated by two models under (a) RCP 8.5 scenario and (b) RCP 2.6 scenario.**

**(a)**

| Average annual carbon fluxes (PgC yr <sup>-1</sup> ) |                     | TEM_Moss | TEM 5.0 | Difference | Moss NPP/ Vascular plants NPP |
|--|---------------------|----------|---------|------------|-------------------------------|
| NPP  | Moss NPP            | 3.84     | -       | -          | 38.4%                         |
|  | Vascular plants NPP | 10       | 12.53   | -          |                               |
|  | Total NPP           | 13.84    | 12.53   | 1.31       |                               |
| $R_H$  |                     | 11.28    | 11.54   | -0.21      |                               |
| NEP  |                     | 2.56     | 0.99    | 1.57       |                               |

**(b)**

| Average annual carbon fluxes (PgC yr <sup>-1</sup> ) |                     | TEM_Moss | TEM 5.0 | Difference | Moss NPP/ Vascular plants NPP |
|--|---------------------|----------|---------|------------|-------------------------------|
| NPP  | Moss NPP            | 3.74     | -       | -          | 40.5%                         |
|  | Vascular plants NPP | 9.24     | 11.52   | -          |                               |
|  | Total NPP           | 12.98    | 11.52   | 1.46       |                               |
| $R_H$  |                     | 10.91    | 11.24   | -0.33      |                               |
| NEP  |                     | 2.07     | 0.28    | 1.79       |                               |

**Table 12. Increasing of SOC, vegetation carbon (VGC), and moss carbon (MOSSC) from 1900 to 2000, and total carbon storage during the 21<sup>st</sup> century predicted by two models under (a) RCP 2.6 scenario and (b) RCP 8.5 scenario.**

**(a)**

| Models   | Carbon pools | Carbon pool amounts in 2000/2099 (units: Pg) | Changes in carbon pools during the 21 <sup>st</sup> century (units: Pg) |
|----------|--------------|--|---|
| TEM_Moss | SOC          | 608.1/692.8                                  | 84.7  |
|          | VEGC         | 320.2/432.8                                  | 112.6   |
|          | MOSSC        | 26.2/35.6                                    | 9.4   |
|          | Total        | 954.5/1161.2                                 | 206.7   |
| TEM 5.0  | SOC          | 604.4/616.5                                  | 12.1  |
|          | VEGC         | 318.2/333.7                                  | 15.5  |
|          | Total        | 922.6/950.2                                  | 27.6  |

**(b)**

| Models   | Carbon pools | Carbon pool amounts in 2000/2099 (units: Pg) | Changes in carbon pools during the 21 <sup>st</sup> century (units: Pg) |
|----------|--------------|--|---|
| TEM_Moss | SOC          | 615.9/708.4                                  | 92.5  |
|          | VEGC         | 327.8/481.4                                  | 153.6   |
|          | MOSSC        | 28.1/38.2                                    | 10.1  |
|          | Total        | 971.8/1228.0                                 | 256.2   |
| TEM 5.0  | SOC          | 610.2/654.4                                  | 44.2  |
|          | VEGC         | 324.9/379.4                                  | 54.5  |
|          | Total        | 935.1/1033.8                                 | 98.7  |